

# Speeding up Learning Quantum States through Group Equivariant Convolutional Quantum Ansätze

Han Zheng,<sup>1,2,\*</sup> Zimu Li,<sup>2,†</sup> Junyu Liu<sup>\*,3,4,5,‡</sup> Sergii Strelchuk,<sup>2,§</sup> and Risi Kondor<sup>1,6,7,¶</sup>

<sup>1</sup>*Department of Statistics, The University of Chicago, Chicago, IL 60637, USA*

<sup>2</sup>*DAMTP, Center for Mathematical Sciences, University of Cambridge, Cambridge CB30WA, UK*

<sup>3</sup>*Pritzker School of Molecular Engineering, The University of Chicago, Chicago, IL 60637, USA*

<sup>4</sup>*Chicago Quantum Exchange, Chicago, IL 60637, USA*

<sup>5</sup>*Kadanoff Center for Theoretical Physics, The University of Chicago, Chicago, IL 60637, USA*

<sup>6</sup>*Department of Computer Science, The University of Chicago, Chicago, IL 60637, USA*

<sup>7</sup>*Flatiron Institute, New York City, NY 10010, USA*

(Dated: January 21, 2022)

We develop a theoretical framework for  $S_n$ -equivariant quantum convolutional circuits, building on and significantly generalizing Jordan’s Permutational Quantum Computing (PQC) formalism. We show that quantum circuits are a natural choice for Fourier space neural architectures affording a super-exponential speedup in computing the matrix elements of  $S_n$ -Fourier coefficients compared to the best known classical Fast Fourier Transform (FFT) over the symmetric group. In particular, we utilize the Okounkov-Vershik approach to prove Harrow’s statement (Ph.D. Thesis 2005 p.160) on the equivalence between  $SU(d)$ - and  $S_n$ -irrep bases and to establish the  $S_n$ -equivariant Convolutional Quantum Alternating Ansätze ( $S_n$ -CQA) using Young-Jucys-Murphy (YJM) elements. We prove that  $S_n$ -CQA are dense, thus expressible within each  $S_n$ -irrep block, which may serve as a universal model for potential future quantum machine learning and optimization applications. Our method provides another way to prove the universality of Quantum Approximate Optimization Algorithm (QAOA), from the representation-theoretical point of view. Our framework can be naturally applied to a wide array of problems with global  $SU(d)$  symmetry. We present numerical simulations to showcase the effectiveness of the ansätze to find the sign structure of the ground state of the  $J_1$ - $J_2$  antiferromagnetic Heisenberg model on the rectangular and Kagome lattices. Our work identifies quantum advantage for a specific machine learning problem, and provides the first application of the celebrated Okounkov-Vershik’s representation theory to machine learning and quantum physics.

\*: corresponding author.

## I. INTRODUCTION

The combination of new ideas from machine learning and recent developments in quantum computing has led to an impressive array of new applications. [1–13]. Prominent examples of interplay are the Variational Quantum Eigensolver (VQE) and Quantum Approximate Optimization Algorithm (QAOA) [14–16], which are considered among the most promising quantum machine learning approaches in the Noisy Intermediate-Scale Quantum (NISQ) [17] era. VQEs and QAOA have shown tremendous promise in quantum simulation and quantum optimization [18–23].

One of the most important neural network architectures in classical machine learning are Convolutional Neural Networks (CNNs) [24–28]. In recent years, CNNs have also found applications in condensed matter physics and quantum computing. For instance, authors

in [29] proposes a quantum convolutional neural network with  $\log N$  parameters to solve topological symmetry-protected phases in quantum many-body systems, where  $N$  is the system size. One of the key properties of classical CNNs is equivariance, which roughly states that if the input to the neural network is shifted, then its activations translate accordingly. Equivariance is one of the main reasons behind the unreasonable success of CNNs. However, when working with discrete representational spaces used to describe finite-dimensional quantum systems, generalizing the classical notion of equivariance becomes challenging.

In quantum systems, there is a discrete set of translations corresponding to permuting the qudits as well as a continuous notion of translation corresponding to spatial rotations by elements of  $SU(d)$ . Combining these two is the basis of so-called Permutational Quantum Computing (PQC) [30]. Therefore, a natural starting point for realizing convolutional neural networks in quantum circuits is to look for *permutational equivariance*. In the most general setting this is somewhat of a daunting task however, since by Cayleigh’s Theorem, it contains as special cases equivariance to any finite group.

In recent years, there has been a surge of interest in designing neural networks that are equivariant to the action of various symmetry groups [31]. In particular, it has been recognized that by constructing neural networks that operate on the basis of irreducible represen-

\* hanz98@uchicago.edu

† lizm@mail.sustech.edu.cn

‡ junyuliu@uchicago.edu

§ ss870@cam.ac.uk

¶ risi@cs.uchicago.edu

tations of the group (so-called Fourier space neural networks), and group equivariant convolution is easy to implement because it simply reduces to matrix multiplication [32]. Such Fourier-space CNNs have seen applications in spherical image recognition [33, 34], chemistry [35, 36] and particle physics [37] (e.g. Lorentz group equivariance). Permutation equivariant networks have been used in the context of learning set-valued functions [38] and learning on graphs [39, 40]. Most applications of permutation-equivariant neural networks work with a subset of representations of  $S_n$ . In contrast, in physical and chemical models where the Hamiltonian exhibits global  $SU(d)$  symmetry, such as the Heisenberg model, it is necessary to consider *all* the  $S_n$  irreps. However, even the best classical Fast Fourier Transform (FFT) over the symmetric group  $S_n$  requires at least  $\mathcal{O}(n!n^2)$  operations [41, 42], which dashes any hope of calculating the Fourier coefficients even for relatively small  $n$ . Indeed, despite increasing realization of the importance of enforcing  $SU(2)$  symmetry, none of the neural-network quantum state (NQS) ansätze are able to respect  $SU(2)$  symmetry for all  $SU(2)$  irreps, due to the super-polynomial growth of the number of multiplicities of irreps and the super-exponential cost to compute Fourier coefficients over  $S_n$ . Finding variational ansätze respecting continuous rotation symmetry is highly desirable because it not only helps to gain important physical insights about the system but also leads to more efficient simulation algorithms [43].

There have been several attempts to introduce theoretically sound analogs of convolutional neural networks to quantum circuits, but they have generally been somewhat heuristic. The major difficulty is that the key ingredient of the success of CNNs – translation invariance – lacks a mathematically rigorous quantum counterpart due to the discrete spectrum of spin-based quantum circuits. For example, [29] uses the quasi-local unitary operators to act vertically across all qubits.

In this paper, we argue that the natural form of equivariance in quantum circuits is permutation equivariance and proposing a broad class of  $k$ -local  $S_n$  equivariant quantum convolutional ansätze. We introduce a theoretical framework to incorporate group-theoretical CNNs into the quantum circuits, building on and generalizing the PQC’s framework. As a feature, the *Schur-Weyl* duality between  $S_n$  and  $SU(d)$  appears naturally and will be used throughout the paper. We rigorously demonstrate the equivalence of labeling Schur basis by YJM-elements and by Casimir operators, first conjectured in Harrow’s thesis [44], (see also discussions by Bacon, Chuang, and Harrow [45] and Krovi [46]), using the Okounkov-Vershik approach [47]. Using the refined duality we show that the quantum circuits are the natural Fourier space in the sense that one does not need to encode Fourier coefficients to perform the *Fourier space  $G$ -equivariance convolution*, with the corresponding initial states, having been prepared using constant-depth qudit circuits. An immediate consequence of this is the existence of a super-

exponential speed-up when evaluating matrix elements of  $S_n$  Fourier coefficients and on performing  $G$ -equivariant convolution via simulating  $k$ -local  $\mathbb{C}[S_n]$  Hamiltonian on qudits. This quantum super-exponential speed-up naturally circumvents the need to perform classical Fourier space activation, suggesting that quantum circuits are well-suited to implement the group-equivariant CNNs.

Motivated by the class of problems with a global  $SU(d)$  symmetry, we construct the variational  $S_n$ -equivariant Convolutional Quantum Alternating ansätze ( $S_n$ -CQA). We show that  $S_n$ -equivariant CQA is dense in every  $S_n$ -irrep, hence it acts as universal variational model for problems that possess global  $SU(2)$  symmetry. A direct consequence of this density result is that  $S_n$ -CQA can be applied to a wide array of machine learning and optimization tasks that exhibit global  $SU(d)$  symmetry or require explicit computation of high dimensional  $S_n$ -irreps, thus presenting a quantum super-exponential speed-up. The proof techniques in the density result of  $S_n$ -CQA are of independent interest and can be applied to the study of computational power of Quantum Adiabatic Optimization Algorithm. The latter is designed to solve combinatorial optimization problems and can be implemented in near-term quantum hardware [16]. It is shown in [48, 49] that QAOA ansätze generated by simple local Hamiltonians are universal. We use our techniques to derive the universality for a different but related class of QAOA ansätze with a richer set of mixer Hamiltonians. In addition, we show that the  $S_n$ -CQA ansätze correspond to a new class of Quantum Adiabatic Optimization Algorithms under the Schur basis, with path dependent coupling strengths for the mixer Hamiltonian.

We illustrate the potential of this framework by applying it to the problem of finding the sign structure of the ground state of  $J_1 - J_2$  antiferromagnetic Heisenberg magnets. This is a paradigmatic case where classical neural networks struggle to discover the sign structure to an admissible accuracy due to violation of global  $SU(2)$  symmetry [50, 51]. We include numerical simulation to show the effectiveness of the  $S_n$ -CQA ansätze in finding the ground state’s sign structure in the frustrated region using only  $\mathcal{O}(pn^2)$  parameters for  $p$  alternating layers.

All statements and theorems discussed in the main text are proved in full detail in Supplementary Material (SM).

## II. REFINED SCHUR-WEYL DUALITY

Schur-Weyl duality is widely used in quantum computing, quantum information theory and high energy physics. In particular, in Quantum Chromodynamics it was used to decompose the  $n$ -fold tensor product of  $SU(3)$  representations. In this context, standard Young tableaux are referred to as Weyl-tableaux and labeled by the three iso-spin numbers  $(u, d, s)$ . The underlying Young diagrams contain three rows  $\lambda = (\lambda_1, \lambda_2, \lambda_3)$  that also correspond to irreps of  $S_n$  via Schur-Weyl duality (Fig.1 & Fig.2 (a), (b)). In physics, the convention is to

use Young diagrams  $\lambda' = (\lambda'_1, \lambda'_2)$  labeled by Dynkin integers via highest weight vectors. Thus Young diagrams are one row shorter than their mathematical counterparts (for any  $SU(d)$ ). We will henceforth adhere to the mathematical notation for the rest of this paper.

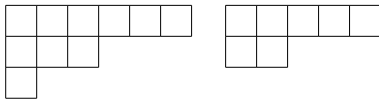


FIG. 1: Mathematical (left) and physical (right) notations of Young diagrams  $\lambda = (6, 3, 1), \lambda' = (5, 2)$  representing to the same  $SU(3)$ -irrep of highest weight  $(3, 2)$ . The mathematical notation also corresponds to an  $S_{10}$ -irrep in Schur-Weyl duality.

### A. Background on the Representation Theory of the Symmetric Group

In this section we define some of the mathematical concepts and notations used in the rest of the paper. Further details can be found in [52–54].

Let  $V$  be a  $d$ -dimensional complex Hilbert space with orthonormal basis  $\{e_1, \dots, e_d\}$ . The tensor product space  $V^{\otimes n}$  admits two natural representations: the *tensor product representation*  $\pi_{SU(d)}$  of  $SU(d)$  acting as

$$\pi_{SU(d)}(g)(e_{i_1} \otimes \dots \otimes e_{i_n}) := g \cdot e_{i_1} \otimes \dots \otimes g \cdot e_{i_n},$$

where  $g \cdot e_{i_k}$  is the fundamental representation of  $SU(d)$ , and *permutation representation*  $\pi_{S_n}$  of  $S_n$  acting as

$$\pi_{S_n}(\sigma)(e_{i_1} \otimes \dots \otimes e_{i_n}) := e_{i_{\sigma^{-1}(1)}} \otimes \dots \otimes e_{i_{\sigma^{-1}(n)}}.$$

**Theorem** (Schur-Weyl Duality). *For all Young diagrams  $\mu, \lambda$  of size  $n$  with at most  $d$  rows,  $\pi_{SU(d)}$  and  $\pi_{S_n}$  can be decomposed as*

$$\pi_{SU(d)} \cong \bigoplus_{\mu} W_{\mu} \otimes 1_{m_{SU(d), \mu}}, \quad \pi_{S_n} \cong \bigoplus_{\lambda} 1_{m_{S_n, \lambda}} \otimes S^{\lambda},$$

where  $W_{\mu}$  denotes an  $SU(d)$ -irrep,  $S^{\lambda}$  denotes the dual  $S_n$ -irrep and  $m_{SU(d), \mu}, m_{S_n, \lambda}$  are multiplicities. With respect to the same Young diagram,  $\dim W_{\lambda} = m_{S_n, \lambda}$  and  $\dim S^{\lambda} = m_{SU(d), \lambda}$  (see for example, Fig.2 (a) and (b)).

One can easily verify that  $\pi_{SU(d)}$  and  $\pi_{S_n}$  commute (further properties are described in the SM). Consider the *symmetric group algebra*  $\mathbb{C}[S_n]$  consisting of all formal finite sums  $f = \sum_i c_i \sigma_i$ . Its representation is then  $\tilde{\pi}_{S_n}(f) = \sum_i c_i \pi_{S_n}(\sigma_i)$ . When there is no ambiguity, we denote by  $U_{\sigma}$  or simply  $\sigma$  the representations  $\pi_{S_n}(\sigma)$ .

Another decomposition that will be important is the decomposition of the so-called *permutation module*  $M^{\mu}$ . Fortunately there is an accessible way to understand  $M^{\mu}$  in the tensor product space  $V^{\otimes n}$ . To make things simpler, consider the  $d = 2$  case of  $SU(2) - S_n$  duality on

$(\mathbb{C}^2)^{\otimes n}$ . Only two-row Young diagrams  $\lambda = (\lambda_1, \lambda_2)$  appear in this duality and the half of difference  $\frac{1}{2}(\lambda_1 - \lambda_2)$  between the lengths of the two rows gives the total spin of the  $SU(2)$ -irrep  $W_{\lambda}$ . The permutation module  $M^{\mu}$  is isomorphic with the linear span of all computational basis vectors with  $z$ -spin components equal to  $\frac{1}{2}(\mu_1 - \mu_2)$ .

Note that,  $(\mathbb{C}^2)^{\otimes n} = \bigoplus_{\mu} M^{\mu}$  and each  $M^{\mu}$  is invariant under  $S_n$  permutation. Furthermore,  $M^{\mu}$  can be further decomposed into  $S_n$ -irreps. For two-row Young diagrams ( $SU(2) - S_n$  duality), the decomposition is easy:  $M^{\mu} = \bigoplus_{\lambda \geq \mu} S^{\lambda}$  where  $\lambda, \mu$  have the same size  $n$  and we use the *dominance order*  $\lambda \geq \mu$  if  $\lambda_1 \geq \mu_1$ . In summary, we have

$$(\mathbb{C}^2)^{\otimes n} = \bigoplus_{\mu} M^{\mu} = \bigoplus_{\mu} \bigoplus_{\lambda \geq \mu} S^{\lambda} \cong \bigoplus_{\lambda} 1_{m_{S_n, \lambda}} \otimes S^{\lambda}.$$

Isomorphic copies of  $S^{\lambda}$  come from different permutation module  $M^{\mu}$ . The largest permutation module contains all distinct  $S_n$ -irreps in  $(\mathbb{C}^2)^{\otimes n}$  (see e.g., Fig.2 (c)). For general Young diagrams, decompositions of  $M^{\mu}$  would have nontrivial multiplicities [52, 54].

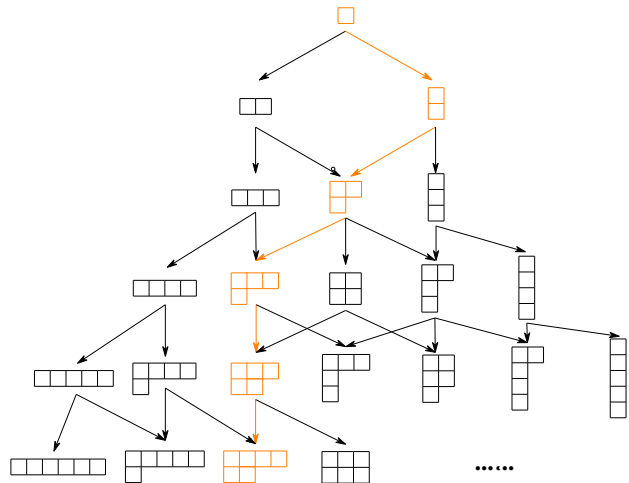


FIG. 3: Bratteli diagram for  $S_6$ . Upper Young diagrams connecting by arrows to lower ones arise from the decomposition. Orange arrows form a path. Note that diagrams with more than two rows cannot appear in  $SU(2) - S_6$  duality.

Each  $S^{\lambda}$  can be decomposed further with respect to  $S_{n-1} \subset S_n$  as  $S^{\lambda} = \bigoplus_{S_{n-1}, \rho} S^{\lambda \rho}$ . The so-called *branching rule* guarantees that the decomposition is multiplicity-free, i.e., distinct  $S_{n-1}$ -irrep  $S^{\lambda \rho}$  appear only once in the decomposition. The so-called Bratteli diagrams in Fig.3 show how different irreps are decomposed. Continuing the decomposition process for  $S_{n-2}, \dots, S_1$ , the original space  $S^{\lambda}$  will be written as a direct sum of 1-dimensional subspaces ( $S_1$ -irreps are 1-dimensional):

$$S^{\lambda} = \bigoplus_{S_{n-1}, \rho} S^{\lambda \rho} = \dots = \bigoplus_{S_{n-1}, \rho} \dots \bigoplus_{S_1, \tau} S^{\lambda \rho \sigma \dots \tau}.$$

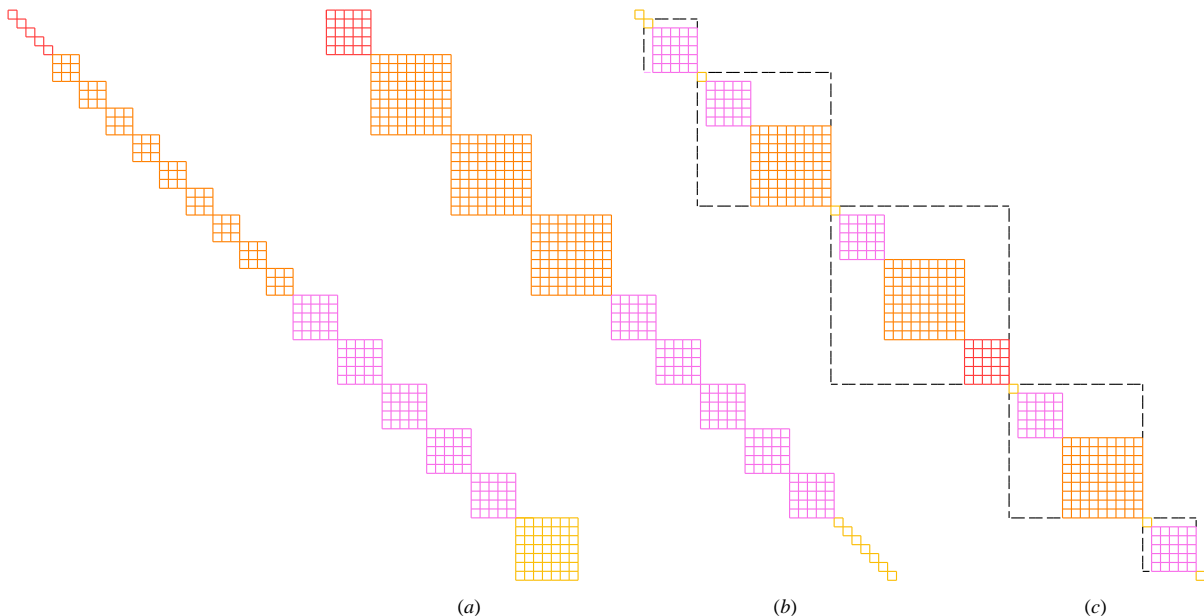


FIG. 2: (a) is the decomposition of  $(\mathbb{C}^2)^6$  with respect to  $SU(2)$  while (b) is for  $S_6$  by Schur-Weyl duality. (c) respects both permutation modules and irreps of  $S_6$ .

Each 1-dimensional subspace  $S^{\lambda\rho\sigma\cdots\tau}$  can be represented by a nonzero vector in it. Normalizing them, we obtain an orthonormal basis  $\{|v_T\rangle\}$  of  $S^\lambda$  called the *Gelfand-Tsetlin basis (GZ)* or *Young-Yamanouchi basis*. Indices  $\lambda, \rho, \sigma, \dots, \tau$  form a path in the Bratteli diagram (see Fig.3) and can be used to define a standard Young tableau  $T$  (Fig.4). Young basis vectors are in one-to-one correspondence with standard Young tableaux [52]. The branching rule is also discussed in  $SU(d)$  representation theory and some authors refer to the  $SU(d)$ -irrep basis as the GZ-basis if it is constructed in a similar manner.

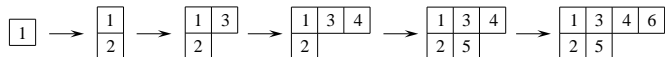


FIG. 4: The Standard Young tableau defined by the path in Fig.3

Let us introduce the central concept used in our work:

**Definition.** For  $1 < k \leq n$ , the *Young-Jucys-Murphy element*, or *YJM-element for short*, is defined as a sum of transpositions  $X_k = (1, k) + (2, k) + \cdots + (k-1, k) \in \mathbb{C}[S_n]$ . We set  $X_1 = 0$  as a convention.

As the name indicates, this concept was developed by Young [55], Jucys [56] and Murphy [57]. Okounkov and Vershik showed that YJM-elements generate the *Gelfand-Tsetlin subalgebra*  $GZ_n \subset \mathbb{C}[S_n]$  [47], which is a maximal commutative subalgebra consisting of all centers  $Z[S_k]$  of  $\mathbb{C}[S_k]$  for  $k = 1, \dots, n$ . Another striking fact is that all YJM-elements are strictly diagonal (indeed, representation of  $GZ_n$  consists of all diagonal matrices) in a Young basis  $\{|v_T\rangle\}$  whose eigenvalues can be read

out directly from the standard Young tableaux  $T$ . To be precise, let  $\lambda$  be a Young diagram. Since this is a 2-dimensional diagram, we can naturally assign integer coordinates to its boxes. The *content* of each of its boxes is determined by the  $x$ -coordinate minus  $y$ -coordinate. Suppose  $T$  is a standard Young tableau of  $\lambda$ . Arranging all contents with respect to  $T$ , we obtain the *content vector*  $\alpha_T$ . For instance, the Young diagram  $\lambda = (4, 2)$  has contents  $0, 1, 2, -1$ . The specific standard tableau  $T$  in Fig.4 has content vector  $\alpha_T = (0, -1, 1, 2, 0, 3)$ . Let  $|v_T\rangle$  denote a Young basis vector corresponding to  $T$ . Measuring by YJM-elements, we have  $X_1 |v_T\rangle = 0$ ,  $X_2 |v_T\rangle = -|v_T\rangle$ ,  $X_3 |v_T\rangle = |v_T\rangle$  and so forth. Each Young basis vector is determined uniquely by its content vector (see [47] and [54] for more details).

## B. Correspondence between Spin Labels and Content Vectors

Working from the perspective of Schur-Weyl duality requires, at least theoretically, using the *Schur basis* rather than the computational basis. As we introduced above, it can be the Young basis constructed by the branching rule of  $S_n$ . However, a more conventional way is conducting sequential coupling and Clebsch-Gordan decompositions of  $SU(d)$  [30, 44, 58]. We now turn to the question whether this  $SU(d)$  irrep basis, labeled by  $d-1$  Casimir operators [59], is the same as the Young basis of  $S_n$  labeled by  $n$  YJM-elements. This was conjectured to be true in [44] and surfaced again in [46] when authors introduced an efficient Quantum Schur Transform (QST). An affirmative answer to this conjecture is cru-



cial in this work for two reasons: (a) The Young basis is algebraic. Thus, the gate action drawing from the group algebra  $\mathbb{C}[S_n]$  is basis-independent. In particular, it can be implemented directly in the computational basis without computing the Fourier coefficients – this is a key observation that underpins the super-exponential quantum speed-up. (b) This identification allows us to efficiently generate quantum states required for optimization and learning tasks. As we will show in Section III B in the qubit case, this initialization will be done using circuits of constant depth.

For two-row Young diagrams, this conjecture was shown to be correct in [60], where the author studies the question by  $\frac{1}{2}$ -spin eigenfunctions instead of YJM-elements. Our first mathematical result shows that the general case for  $SU(d) - S_n$  duality still holds and can be proven in a surprisingly easy way using YJM-elements and the Okounkov-Vershik approach. The proof is presented in the SM.

**Lemma 1.** *Under  $SU(d) - S_n$  duality, sequentially coupled Casimir operators commute with YJM-elements.*

To illustrate this result, consider the *sequentially coupled total spin basis*  $|j_1, j_2, \dots, j_{n-1}, j_n, m\rangle$  of  $SU(2)$ . The *spin component*  $m$  and *spin labels*  $j_k$  are determined by spin operator  $S_z^n = \sum_{i=1}^n S_i^z$  and sequential coupled Casimir operators  $J_k^2 = (S_x^k)^2 + (S_y^k)^2 + (S_z^k)^2$  respectively. Since they commute with YJM-elements,  $J_k^2 X_i |j_1, j_2, \dots, j_{n-1}, j_n, m\rangle = X_i J_k^2 |j_1, j_2, \dots, j_{n-1}, j_n, m\rangle$ . We thus arrive at the following result:

**Theorem 1.** *YJM-elements are strictly diagonal under the  $SU(d)$  irrep basis. Conversely, sequentially coupled Casimir operators are strictly diagonal under the Young basis. Hence the  $SU(d)$  irrep basis and the Young basis are equivalent.*

We henceforth denote both bases with unifying notation  $|v_T^\mu\rangle$ , where the subscript  $T$  denotes a standard Young tableau, or equivalently the corresponding GZ-path from the Bratteli diagram, and the superscript  $\mu$ , as explained in Section II A, comes with the permutation module  $M^\mu$ . An example in the next paragraph shows that basis vectors with the same subscript  $T$  but different superscripts  $\mu$  come from multiple copies of an  $S_n$ -irrep. We do not need to distinguish these copies mostly except in Section III B, so the superscript  $\mu$  will often be omitted. A detailed study on labeling multiple  $SU(d)$  states can be found in [61].

At the end of this section, we illustrate diagrammatically the correspondence between spin labels and content vectors as a corollary of the preceding theorem plus Schur-Weyl duality. For brevity, consider  $|v_T\rangle$  from Fig. 4. Its content vector  $\alpha_T$  equals  $(0, -1, 1, 2, 0, 3)$ . The first spin-label is definitely  $j_1 = \frac{1}{2}$ . Because  $|v_T\rangle$  is both a Young basis element and a total spin state, the next spin label should also be recorded according to the path in Fig. 4. That is,  $j_2 = j_1 + \frac{1}{2}$  if the box containing 2

is put in the first row of the Young diagram. Otherwise, we subtract  $\frac{1}{2}$ . Consequently, we obtain spin labels  $(\frac{1}{2}, 0, \frac{1}{2}, 1, \frac{1}{2}, 1)$ . Since the total spin (last spin label) of  $|v_T^\mu\rangle$  is 1, there are three possible choices of  $z$ -spin components  $j = 1, 0, -1$  and they can be found in three different permutation modules (Fig. 2 (c)). The largest one takes  $|v_T^0\rangle$  with  $\mu = (3, 3)$ . Note that the pattern of constructing  $SU(2)$  spin labels is simply the familiar branching rule seen in  $SU(2)$ -irreps [62]. This pattern still holds for spin label-content vector correspondence in  $SU(d)$  case. The refined Schur-Weyl duality by incorporating the equivalence between  $SU(d)$  irrep bases and the Young bases is at the heart of the quantum Schur transform. Furthermore, in the following sections, we show how the refined Schur-Weyl duality leads to a quantum super-exponential speed-up in performing  $S_n$  equivariant quantum convolutions which can be applied to a wide array of quantum machine learning and optimization tasks.

### III. QUANTUM CIRCUITS AS NATURAL FOURIER SPACE

Following [63, 64], given a compact group  $G$ , it is tempting to implement  $G$ -equivariant convolutions in the quantum circuits, where the equivariance property is given in the corresponding group algebra  $L^2(G, *)$  equipped with convolution operator  $*$ . For  $f_1, f_2 \in \mathbb{C}[S_n]$ :

$$(f_1 * f_2)(\sigma) \equiv \sum_{\tau \in S_n} f_1(\tau) f_2(\tau^{-1}\sigma), \quad (1)$$

where the equivariance is defined with respect to the left action  $L_\eta$  on  $\mathbb{C}[S_n]$ :

$$L_\eta(f_1 * f_2)(\sigma) = (L_\eta f_1 * f_2)(\sigma) = (f_1 * f_2)(\eta^{-1}\sigma).$$

On the other hand, just like the case of  $S_n$ , any representation  $(\pi_G, V)$  can be extended to the group algebra by defining  $\tilde{\pi}_G(f) = \sum_{g \in G} f(g)\pi(g)$ , which is a homomorphism with respect to the convolution:  $\tilde{\pi}_G(f_1 * f_2) = \tilde{\pi}_G(f_1)\tilde{\pi}_G(f_2)$  [53] (RHS is a matrix product). Therefore, the so-called equivariance property is just the associativity of  $\tilde{\pi}_G$  on the representation space or Fourier space in the sense that  $\tilde{\pi}_G(f)$  encodes Fourier coefficients of  $f$  [63, 64]. In what follows, this perspective will be applied to  $S_n$  representation in the context of a recently studied computational model.

Permutational Quantum Computing (PQC) [30] takes inspiration from Topological Quantum Computing (TQC) and Penrose spin network model [65]. In particular, PQC can be seen to mimic some features of TQC, where total spin bases play the role of anyons and computation proceeds by qubit interchange and spin measurement. Suppose we prepare an appropriate Young basis element  $|v_T\rangle = U_{\text{Sch}}|x\rangle$  for some  $x \in \{0, 1\}^n$ , where  $U_{\text{Sch}}$  is the quantum Schur transform (QST) in

qudits and  $\mu$  is the corresponding  $SU(d)$  label (Dynkin integer), such that we can measure the matrix elements:  $\langle v_{T'} | \pi(\sigma) | v_T \rangle$ . Using  $\mathcal{O}(n^2)$  SWAP gates, Jordan argues that the measurements form the permutational quantum polynomial (PQP) class [30]. Capable of computing the matrix elements of the  $S_n$ -irreps in polynomial time was conjectured to capture the non-classical aspects of quantum computing. However, a classical sampling method was later found in [58] for qubits. In this work, we extend the class of PQP (for which we call PQP+) in the hope to capture some of the non-classical aspects by extending  $\pi$  as the algebra homomorphism  $\tilde{\pi}(f)$  for some  $f = \sum c_i \sigma_i \in \mathbb{C}[S_n]$ . To be specific, consider a class of problems that can be solved by measuring

$$\langle v_{T'} | \tilde{\pi}(f) | v_T \rangle := \sum c_i \langle v_{T'} | \pi(\sigma_i) | v_T \rangle.$$

in polynomial time via Fourier space convolution. In particular, we define PQP+ by the set of polynomially-bounded quantum algorithms able to approximate the matrix elements of the so-called Hamiltonian simulation in qudits:

$$\begin{aligned} \exp(-i\tilde{\pi}(f)) &= \sum_{n=0}^{\infty} \frac{(-i)^n}{n!} (\tilde{\pi}(f))^n \\ &= \sum_{n=0}^{\infty} \frac{(-i)^n}{n!} \underbrace{\tilde{\pi}(f * \dots * f)}_{n \text{ many}}. \end{aligned} \quad (2)$$

Note that the Wedderburn theorem implies that Equation (2) encompasses all *unitary*  $S_n$ -Fourier coefficients. If  $f$  is supported on  $k$ -qubits (acting on arbitrary  $k$  qubits), so is its auto-correlation  $f * \dots * f$ , and we can efficiently simulate it using standard Hamiltonian simulation methods. The corresponding Hamiltonian evolution need not be  $k$ -local, and there is an efficient quantum Schur transform proposed with gate complexity  $\text{Poly}(n, \log d, \log(1/\epsilon))$  [44–46]. Thus, it follows that the  $\mathbb{C}[S_n]$  generalization to PQC is able to achieve super-exponential speed-up computing the matrix element of  $\mathbb{C}[S_n]$  Fourier coefficients of the following form, where no polynomial-time classical algorithm is found.

**Theorem 2.** *Consider a  $k$ -local  $\mathbb{C}[S_n]$  Hamiltonian  $H = \tilde{\pi}(f)$  with Young basis elements  $|v_T\rangle, |v_{T'}\rangle$  prepared using the efficient high dimensional QST. The quantum circuit of qudits is able to simulate the matrix element:*

$$\langle v_{T'} | \exp(-itH) | v_T \rangle = \delta_{T',T} \langle v_{T'} | \exp(-itH) | v_T \rangle,$$

in  $\mathcal{O}\left(tCk^3n^k \frac{\log(tCkn^k/\epsilon)}{\log \log(tCkn^k/\epsilon)}\right)$  SWAP gates with the constant  $C = \max_i |c_i|$ .

*Proof.* The proof is based on the method of Linear Combination Unitaries (LCU) from [66]. First, we determine the operator norm of  $H$ . A standard result for the symmetric group  $S_n$  is that the number of permutations supported exactly on  $l$  elements, or equivalently with  $n-l$

elements being fixed is calculated by the *derangement*:

$$D_l = \frac{n!}{(n-l)!} \left( \frac{1}{2!} - \frac{1}{3!} + \dots + (-1)^l \frac{1}{l!} \right).$$

When  $H$  is  $k$ -local, then it contains at most  $D_2 + \dots + D_k$  different permutations from  $S_n$ . Since  $n!/(12(n-l)!) \leq D_l \leq n!/(4(n-l)!)$ , the number is of order  $\mathcal{O}(kn^k)$ . With  $C = \max_i |c_i|$ ,  $\|H\| = \|\sum c_i \sigma_i\| \leq \mathcal{O}(Ckn^k)$ .

Consider the Hamiltonian simulation via the product formula:

$$[\exp(-i\Delta t H)]^M = \exp(-itH),$$

where we set  $M = tCkn^k$  so that  $\Delta t \|H\| = t\|H\|/M = \mathcal{O}(1)$ . In order to bound the total error by  $\epsilon$ , each product term should be simulated within error  $\tilde{\epsilon} = \epsilon/M$ . Then following [66] we take the truncated Taylor series of Equation (2) to order  $K$  such that

$$\|\exp(-i\Delta t H) - \sum_{k=0}^{K-1} \frac{(-i\Delta t H)^k}{k!}\| = \frac{(\Delta t \|H\|)^K}{K!} \leq \tilde{\epsilon}.$$

Using  $(k/e)^k \leq k!$ , the above inequality holds when  $K \log(K/\Delta t \|H\| e) \geq \log(1/\tilde{\epsilon})$ . Since  $\Delta t \|H\| = \mathcal{O}(1)$ , we can further relax the condition to require  $K \log K \geq \log(1/\tilde{\epsilon})$ . Let  $K' := \frac{\log 1/\tilde{\epsilon}}{\log \log 1/\tilde{\epsilon}}$ . Then

$$K' \log K' \geq \log \frac{1}{\tilde{\epsilon}} - \log \frac{1}{\tilde{\epsilon}} \frac{\log \log 1/\tilde{\epsilon}}{\log \log \log 1/\tilde{\epsilon}} \approx \log \frac{1}{\tilde{\epsilon}}$$

for small  $\tilde{\epsilon}$ . Setting  $K = K'$  this bound also recovers the result from [67].

The Taylor expansion gives that:

$$\begin{aligned} \exp(-i\Delta t H) &= \sum_{m=0}^{\infty} \sum_{i_1, \dots, i_m} \frac{(-i\Delta t)^m}{m!} c_{i_1} \dots c_{i_m} \sigma_{i_1} \dots \sigma_{i_m} \\ &= \sum_{m=0}^K \sum_{i_1, \dots, i_m} \tilde{c}_{i_1 \dots i_m} \tilde{\sigma}_{i_1, \dots, i_m} + \mathcal{O}(\tilde{\epsilon}), \end{aligned}$$

where  $N = \mathcal{O}(kn^k)$  is the total number of  $k$ -local permutations and  $c_i$  is the corresponding coefficients with  $\|c_i\| \leq Ckn^k$ . To apply the LCU, we also set:

$$\tilde{c}_{i_1 \dots i_n} = \frac{(\Delta t)^n}{n!} c_{i_1} \dots c_{i_n}, \quad \tilde{\sigma}_{i_1, \dots, i_n} = (-i)^n \sigma_{i_1} \dots \sigma_{i_n}.$$

We need  $\mathcal{O}(\log NK)$  many selection ancilla qubits to implement  $\exp(-i\Delta t H)$  using:  $\mathcal{O}(\exp(\Delta t \|c_i\|_1)) \approx \mathcal{O}(1)$  applications of oblivious amplitude amplification. Since any  $k$ -local permutation  $\sigma_i$  can be written in  $\mathcal{O}(k^2)$  SWAPs, the total circuit complexity is:

$$\mathcal{O}\left(tCk^3n^k \frac{\log(tCkn^k/\epsilon)}{\log \log(tCkn^k/\epsilon)}\right).$$

□

Note that in our work we assume that qudit SWAP gates are easy to implement with constant overhead. We can thus disregard the polynomially-scaling constant on  $k$  in the approximation and write the total circuit complexity  $\mathcal{O}(tn^k \log(tn^k/\epsilon)/\log \log(tn^k/\epsilon))$ . Theorem 2 establishes a generic quantum super-exponential speed-up. We also present a practically relevant quantum super-exponential speed-up for qubits using the following beautiful identity:

$$\pi((ij)) = 2\hat{S}_i \cdot \hat{S}_j + \frac{1}{2}I, \quad (3)$$

where  $\hat{S}_i$  is further expanded as the half of standard Pauli operators  $\{X, Y, Z\}$ . For example, consider  $f = (12) + (23) + (34) + (41)$ . Therefore under  $\tilde{\pi}$ ,

$$H_P \equiv \tilde{\pi}(f) = 2(\hat{S}_1 \cdot \hat{S}_2 + \hat{S}_2 \cdot \hat{S}_3 + \hat{S}_3 \cdot \hat{S}_4 + \hat{S}_4 \cdot \hat{S}_1 + I),$$

where  $H_P$  is simply the 1D Heisenberg chain with a periodic boundary condition of 4 spins. Equation (3) was first discovered by Heisenberg himself [68, 69] (an elementary proof can be found in SM) and more recently noted by [70] in analyzing the ground state property of 1-D Heisenberg chain using symmetry adapted VQE. This identity also supports our numerical simulation on 2-D Heisenberg model in Section VI.

**Theorem 3.** *Suppose  $f \in \mathbb{C}[S_n]$  is  $k$ -local. Consider  $H = \tilde{\pi}(f)$  together with states  $|v_T\rangle, |v_{T'}\rangle$ . The quantum circuit can simulate the matrix elements:*

$$\langle v_{T'} | \exp(-itH) | v_T \rangle = \delta_{T',T} \langle v_{T'} | \exp(-itH) | v_T \rangle,$$

using  $\mathcal{O}\left(tL(k)n^k \frac{\log(tL(k)n^k/\epsilon)}{\log \log(tL(k)n^k/\epsilon)}\right)$  Pauli gates, with the constant  $L(k) = \max_i |c_i| 2^{-1+k}$ .

*Proof.* Since  $f = \sum c_i \sigma_i$  is  $k$ -local, each  $\sigma_i$  acts on at most  $k$  qubits and can be expanded by at most  $k-1$  adjacent transpositions  $\prod_{j=1}^{k-1} \tau_{ij}$ . By Equation (3), it equals

$$\begin{aligned} & \prod_{j=0}^{k-1} (2\hat{S}_{i_j} \cdot \hat{S}_{i_{j+1}} + \frac{1}{2}I) \\ &= \sum_{j=0}^{k-1} \binom{k-1}{j} 2^{k-1-2j} \underbrace{(\hat{S}_{i_1} \cdot \hat{S}_{i_2}) \circ \dots \circ (\hat{S}_{i_{k-1}} \cdot \hat{S}_{i_k})}_{j \text{ many terms replaced by } I}. \end{aligned} \quad (4)$$

The operator norm of  $\hat{S}_{i_j} \cdot \hat{S}_{i_{j+1}}$  can be seen directly from Equation (3) as  $\frac{3}{4}$ . Therefore,

$$\|\sigma_i\| \leq \sum_{j=0}^{k-1} 2^{k-1-2j} \left(\frac{3}{4}\right)^{k-1-j} \binom{k-1}{j} = 2^{k-1},$$

where the last step uses binomial theorem. By Theorem 2,  $H$  contains at most  $\mathcal{O}(kn^k) \sim \mathcal{O}(n^k)$  many  $k$ -local

permutations and hence written explicitly in  $k$ -local Pauli gates:

$$\|H\| \leq \sum_i^{\mathcal{O}(n^k)} L(k) = n^k L(k), \quad (5)$$

where  $L(k) = \max(c_i) 2^{-1+k}$ . The operator norm of  $H$  is thus bounded by  $n^k L(k)$ . The larger bound here reflects the fact that we are using  $k$ -local Pauli gates, whose coefficient 1-norm is also bounded by the above expression. Suppose the complete expansion of  $H$  by Pauli gates is  $\sum_i \beta_i H_i$  with  $H_i$  being products of  $k$ -local Pauli gates like in Equation (4). Then the Taylor expansion gives that:

$$\begin{aligned} \exp(-i\Delta t H) &= \sum_{n=0}^N \sum_{i_1, \dots, i_n} \frac{(-i\Delta t)^n}{n!} \beta_{i_1} \dots \beta_{i_n} H_{i_1} \dots H_{i_n} \\ &= \sum_{n=0}^K \sum_{i_1, \dots, i_n} \tilde{\beta}_{i_1 \dots i_n} \tilde{H}_{i_1, \dots, i_n} + \mathcal{O}(\tilde{\epsilon}), \end{aligned}$$

where  $N = \mathcal{O}(k^2 n^k 4^k)$  is the total count of Pauli operators and  $\beta_i$  is the corresponding coefficients with  $\|\beta_i\| \leq L(k)n^k$  by Equation (5).

Applying the technique of LCU as in Theorem 2, we need  $\mathcal{O}(\log NK)$  many selection ancilla qubits to implement  $\exp(-i\Delta t H)$  using:  $\mathcal{O}(\exp(\Delta t \|\beta_i\|_1) \approx \mathcal{O}(1))$  applications of oblivious amplitude amplification. For each selection, we need at most  $\mathcal{O}(K)$  times of implementation of  $k$ -local Pauli operators. Therefore, the total circuit complexity is simply:

$$\mathcal{O}\left(M \frac{\log(M/\epsilon)}{\log \log(M/\epsilon)}\right) = \mathcal{O}\left(tL(k)n^k \frac{\log(tL(k)n^k/\epsilon)}{\log \log(tL(k)n^k/\epsilon)}\right).$$

This finishes the proof.  $\square$

A more involved derivation using Pauli gates in Theorem 3 in the form of unitary coupled clusters suggests a potentially hardware-friendly implementation on quantum computers [71]. However, the bounds become loose as  $L(k)$  grows exponentially with  $k$ . However, we show that, for any practical application of quantum machine learning and optimization tasks,  $k$  can be taken small, for instance 4-local in the case of solving the Heisenberg model in Section IV and VI.

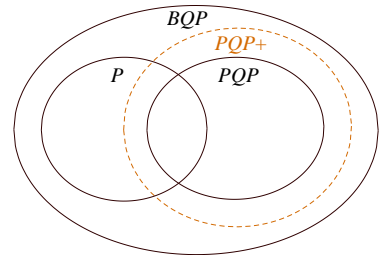


FIG. 5: The relationship between complexity classes. It is not known whether PQP+ strictly contains PQP.

Our results strongly suggest that the PQP+ class is able to capture some non-classical aspects of quantum computation in the qudit case. The above form of  $\mathbb{C}[S_n]$  Hamiltonian simulation by Equation (3) encompasses a large class of physically relevant problems, such as the Heisenberg spin model. Naturally, multiplication of  $\mathbb{C}[S_n]$  Hamiltonian operators correspond to  $\mathbb{C}[S_n]$  convolution, which leads to further useful applications of machine learning and optimization tasks. In what follows, we focus on utilizing the quantum super-exponential speed-up to address quantum machine learning tasks by designing alternating variational  $S_n$  equivariant convolution ansätze. From this point of view, PQP+ may be interpreted as the natural complexity class for *quantum  $S_n$ -Fourier space activation* for quantum machine learning and optimization tasks.

### A. $S_n$ Equivariant Convolutional Quantum Alternating Ansätze

Consider the YJM-elements  $\{X_1, \dots, X_n\}$  introduced in Section II A which generate the maximally commuting subalgebra  $\text{GZ}_n$ . These elements take the Young basis, which is equivalent to any sequential coupled  $\text{SU}(d)$ -irrep basis by Theorem 1, as their common eigenbases. Eigenvalues can be read off directly by the associated content vectors [47]. The use of YJM-elements allows us to design the following *mixing Hamiltonian*:

$$H_M = \sum_{i_1, \dots, i_N} \beta_{i_1 \dots i_N} X_{i_1} \cdots X_{i_N}. \quad (6)$$

The YJM-Hamiltonian is still strictly diagonal in the Young basis. Suppose we can initialize any Young basis element  $|\Psi_{\text{init}}\rangle$  from  $S_n$ -irreps via QST. The following ansatz is developed in the form similar to that of QAOA (Pauli  $X$  is diagonal wrt.  $|+\rangle^{\otimes n}$ ) [16],

$$\cdots \exp(-iH_M) \exp(-i\gamma H_P) \exp(-iH_M) \exp(-i\gamma' H_P) \cdots$$

To be specific, we have defined a family of mixing operators  $H_M$  parameterized by  $\beta_{i_1 \dots i_N}$  that is diagonal in the Young basis, which naturally preserves each  $S_n$ -irrep determined by the initialized states. Differing from the original purpose of using QAOA to solve constraint satisfaction problem, our  $S_n$  Equivariant Convolutional Quantum Alternating Ansätze ( $S_n$ -CQA) are applied to solve problems with global  $\text{SU}(d)$  symmetry or explicitly exhibits permutation equivariance, as long as the problem Hamiltonian can be efficiently simulated in quantum circuits. Indeed, most physical examples involve only 2 or 3 local spin-interactions such as the Heisenberg model studied in Section VI, thus by Theorem 3 can be efficiently simulated.

The  $k$ -dependent constant in Theorems 2 and 3 has, unfortunately, exponential scaling. So in practice, we would like to have perhaps at most 3 or 4-local terms for Hamiltonian simulation in ansätze. We focus on the

following mixing Hamiltonian consisted of only first and second order products of YJM-elements:

$$H_M = \sum_{k \leq l} \beta_{kl} X_k X_l, \quad (7)$$

whose evolution can be efficiently simulated in  $\mathcal{O}(n^4 \log(n^4/\epsilon)/\log \log(n^4/\epsilon))$ . In the next section, we prove that with a mixture as in the Equation (7), the  $S_n$ -CQA ansätze are *dense*: they are able to approximate any unitary from every  $S_n$ -irrep block (Fig.2 (b)). This can be seen as a restricted version of universal quantum computation to  $S_n$ -irreps. Since the 4-local  $S_n$ -CQA is an all-you-need approximation algorithm within PQP+, it is strongly suggestive that the new PQP+ class contains circuits that can approximate matrix elements of all the  $S_n$  Fourier coefficients, for a polynomial length of alternating layer  $p$ . Moreover, the 4-local  $S_n$ -CQA is also the universal tool to approximate the solution of the problem with global  $\text{SU}(d)$  symmetry, such as the Heisenberg models, due to its nature as variational ansätze.

### B. State Preparation for $S_n$ -CQA Ansätze

To investigate evaluation of the matrix elements of  $S_n$  Fourier coefficients, we were confined to the Young basis, which requires the implementation of QST [44–46]. However, for a wide variety of quantum machine learning and optimization tasks, such as determining the ground state sign structure of frustrated magnets, it is often advantageous to relax the constraints and ask how easy it is to initialize the states that live in any given  $S_n$ -irrep. An algorithm to initialize a state in  $(\frac{n}{2}, \frac{n}{2})$ -irrep is given in [70]. We generalize this result to an arbitrary  $S_n$ -irrep even in  $\text{SU}(d) - S_n$  duality. The key is to utilize different permutation modules and multiplicities of  $S_n$ -irreps as in Fig.2 (c). The construct the algorithm inductively: first consider the  $\text{SU}(2) - S_n$  duality in which a  $(\lambda_1, \lambda_2)$ - $S_n$ -irrep is dual to  $\frac{1}{2}(\lambda_1 - \lambda_2)$ - $\text{SU}(2)$ -irrep. Let

$$|\Psi_{\text{init}}\rangle = \underbrace{|0 \cdots 0\rangle}_{k \text{ many}} \otimes \underbrace{|s\rangle \otimes \cdots \otimes |s\rangle}_{\frac{n-k}{2} \text{ many}}, \quad (8)$$

where  $|s\rangle = \frac{1}{\sqrt{2}}(|01\rangle - |10\rangle)$  is one of the Bell states and we assume  $n - k$  is even. Then we have

**Lemma 2.** *Let  $\mu = \lambda = (\frac{n+k}{2}, \frac{n-k}{2})$ . The initialized state  $|\Psi_{\text{init}}\rangle$  is contained in  $S^\lambda$  and belongs to the permutation module  $M^\mu$ .*

*Proof.* Acting by the spin operator  $S^z = \sum_i S_i^z$ , it is easy to check that the spin component of  $|\Psi_{\text{init}}\rangle$  equals  $j = k/2$  hence it belongs to  $M^\mu$ . By Theorem 1, it can be expanded by total spin basis/Young basis elements from  $M^\mu$ . Thus  $|\Psi_{\text{init}}\rangle = \sum_T \alpha_T |v_T^j\rangle$ . Since  $J_+ |\Psi_{\text{init}}\rangle = 0$ , the above summation only takes elements with total spin equal to  $j$  and all these  $|v_T^j\rangle$  with nonzero coefficients are highest weight vectors relative to  $\text{SU}(2)$ . Therefore the result follows by Schur-Weyl duality.  $\square$



We illustrate how to expand  $|\Psi_{\text{init}}\rangle$  as a linear combination of Young basis elements by providing several examples: (a) let  $|\Psi_{\text{init}}\rangle = |s\rangle^{\otimes \frac{n}{2}}$ . This is the state used in [70]. One can check by YJM-elements that it is exactly a Young basis element. (b) for a more involved case, consider the  $(4, 2)$ -irrep of  $S_6$  and write:

$$\begin{aligned} |\Psi_{\text{init}}\rangle &= |00\rangle \otimes |s\rangle \otimes |s\rangle \\ &= \frac{2}{3} |v_{T_1}\rangle - \frac{\sqrt{2}}{3} |v_{T_2}\rangle - \frac{\sqrt{2}}{3} |v_{T_3}\rangle + \frac{1}{3} |v_{T_4}\rangle, \end{aligned}$$

where  $|v_{T_i}\rangle$  are Young basis elements with paths  $T_i$  determined by the branching rule in Figure 6.

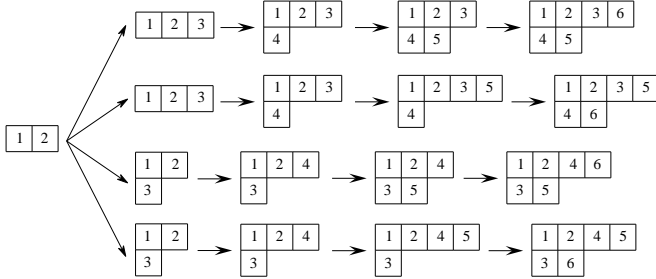


FIG. 6: Decomposing the initial state by content vectors/spin labels.

Let  $|v_T\rangle$  be a Young basis element of  $S_{n-2}$ . To be consistent with the above lemma,  $|v_T\rangle$  is assumed to be the highest weight vector of total spin  $j$ . Tensoring with the singlet  $|s\rangle$  and decomposing via Clebsch-Gordon rule,  $|v_T\rangle \otimes |s\rangle$  is spanned by two highest weight vectors of total spin  $j \pm \frac{1}{2}$ . Then the spin label-content vector duality in Section II B yields the above branches. Moreover, by re-ordering the tensor products of  $|0 \cdots 0\rangle$  and  $|s\rangle$  in Eq.(8) yields different types of linear combinations of Young Bases. By checking the Clebsch-Gordon rule and Bratteli diagram, it is easy to see that each re-ordering yields a different expansion of Young basis elements. Fig.7 illustrates two more cases of  $|s\rangle \otimes |0\rangle \otimes |s\rangle \otimes |0\rangle$  and  $|s\rangle \otimes |00\rangle \otimes |s\rangle$ .

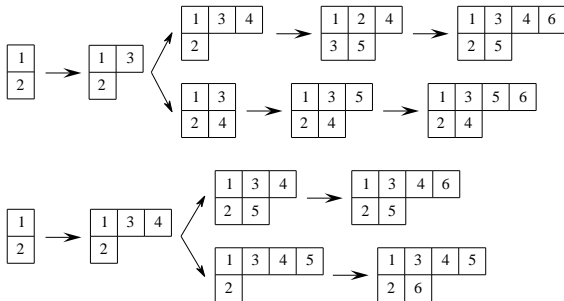


FIG. 7: Reordering tensor products yields different Young basis expansions.

This method can be generalized to  $SU(d) - S_n$  duality. For instance, when  $d = 3$  to initialize states for three-row

Young diagrams, let us consider the upper, down, strange states  $u, d, s$  of  $SU(3)$ . Let

$$|\Psi_0\rangle = \underbrace{|u \cdots u\rangle}_{k \text{ many}} \otimes \underbrace{(ud - du) \otimes \cdots \otimes (ud - du)}_{\frac{n-k}{2} \text{ many}}.$$

This state lies in the  $(n+k, n-k, 0)$ -irrep. Tensoring with  $SU(3)$ -singlet  $|s\rangle = \frac{1}{\sqrt{6}}(uds - usd + dsu - dus + sud - sdu)$ ,  $|\Psi_{\text{init}}\rangle = |\Psi_0\rangle \otimes |s\rangle^{\otimes l}$  is a state from the  $(n+k+l, n-k+l, l)$ -irrep. Its expansion can still be tracked by the branching rule as in Fig. 6 & 7.

#### IV. $S_n$ -CQA ANSÄTZE IS DENSE IN $S_n$ IRREPS

In this section, we show that the  $S_n$ -CQA ansätze are dense in every  $S_n$ -irrep. This restricts universal quantum computation on  $U(d^n)$  to  $S_n$ -irrep blocks (Fig.2 (b)) because our ansätze preserve  $SU(d)$  symmetry. This is of interest for three reasons: (a) the density result indicates that  $S_n$ -CQA ansätze is an universal approximator in PQP+ and it is the theoretical guarantee of our numerical simulations. (b) Similarly to all above theorems, the result is still valid for qudits under  $SU(d) - S_n$  duality. We exhibit again the advantage of working with the symmetric group  $S_n$  as there is no need to deal with complicated  $SU(d)$ -generators in the proof. (c) When changed from Young basis to computational basis, our results form a new proof to the universality of a broad class of QAOA ansätze.

Mathematically, we aim to show that the subgroup generated by  $S_n$ -CQA ansätze is dense in  $U(\dim S^\lambda)$ . However, arguing directly on the level of the Lie group is complicated. Instead, we prove that the generated Lie algebra is isomorphic with  $\mathfrak{u}(\dim S^\lambda)$ . Then combining with some well-known results from the Lie group, we complete the proof. Let us first consider a general lemma where we recall some facts from Cartan subalgebra and root system. The key observation we will rely on is the fact that one can generate a semi-simple Lie algebra only by two elements [72]. Our case is somewhat different: we will first work on the complex general linear algebra  $\mathfrak{gl}(d, \mathbb{C})$  which is not semi-simple, but it is easy to find its Cartan subalgebra – the collection  $\mathfrak{d}(d)$  of all diagonal matrices. Let  $A$  be a matrix with nonzero off-diagonal elements  $c_{ij}$ . It can be thought of as a perturbation from  $\mathfrak{d}(d)$ . We want to know how large the subalgebra generated by  $A$  and  $\mathfrak{d}(d)$  would be. More precisely:

**Lemma 3.** *Let  $E_{ij} \in \mathfrak{gl}(d, \mathbb{C})$  be the matrix unit with entry 1 at  $(i, j)$  and 0 elsewhere. Given any matrix  $A$ , let  $\mathcal{I} \subset \{1, \dots, d\} \times \{1, \dots, d\}$  be the index set of  $A$  assigned with nonzero off-diagonal entries  $c_{kl}$ . Then the Lie subalgebra generated by  $\mathfrak{d}(d)$  and  $A$  contains*

$$\mathfrak{d}(d) \bigoplus_{(i,j) \in \mathcal{I}} R_{ij},$$

where  $R_{ij}$  is the 1-dimensional root space spanned by  $E_{ij}$ .

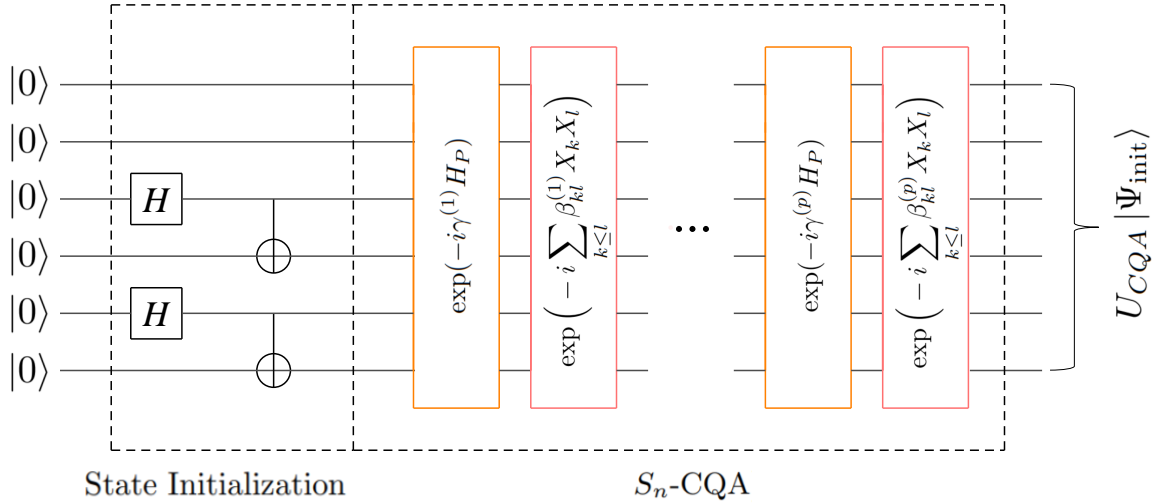


FIG. 8:  $S_6$ -CQA circuit with state initialization in Fig.6.

Proofs in this subsection are rather technical and we relegate them to the SM. Intuitively speaking, the  $GZ_n$  defined in Section II A corresponds precisely to the Cartan subalgebra of  $\mathfrak{gl}(\dim S^\lambda, \mathbb{C})$ . We also want to emphasize that to compute the root  $a_{kl}$  of  $E_{kl}$  under  $GZ_n$ , YJM-elements are not enough. We need a complete span set consisting of all high-order products  $X_{i_1} \cdots X_{i_N}$  and that pose the problem for a practical ansatz design, which requires  $k$ -local  $\mathbb{C}[S_n]$  Hamiltonian in order to be efficiently simulated by quantum circuits (Theorem 2). By basic Lie algebra theory, a root  $a_{kl}$  is computed by Lie brackets  $[X_{i_1} \cdots X_{i_N}, E_{kl}]$ . Since  $|v_T\rangle = \alpha_T(i)|v_T\rangle$  for  $i = 1, \dots, n$  with  $\alpha_T$  as the content vector,  $a_{kl}(i) = [X_i, E_{kl}] = \alpha_{T_k}(i) - \alpha_{T_l}(i)$ . Components of  $a_{kl}$  under  $X_{i_1} \cdots X_{i_N}$  are obtained by taking products of content vectors.

The problem Hamiltonians  $H_P$  of interest are complicated in general and hard to diagonalize classically. In our discourse, we require  $H_P$  to be *path-connected*. A Hamiltonian is of this kind if its associated index graph  $\mathcal{G}_{H_P}$  is connected. For example, the Pauli  $X$  and  $Y$  are path-connected while  $Z$  is not. This condition will be discussed further after Theorem 5 as well as in Section VI. Path-connectedness is also seen in the famous Perron-Frobenius theorem and applied to graph theory.

**Lemma 4.** *Let  $H_P$  be a path-connected Hamiltonian. Then the generated Lie algebra  $\langle \mathfrak{d}(d), H_P \rangle = \mathfrak{gl}(d, \mathbb{C})$ . Consider  $\mathfrak{d}_{\mathbb{R}}(d)$  consisting of all real-valued diagonal matrices. Generated over  $\mathbb{R}$ ,  $\langle i\mathfrak{d}_{\mathbb{R}}(d), iH_P \rangle_{\mathbb{R}} = \mathfrak{u}(d)$ .*

With respect to the Young basis, YJM-elements with their high-order products have real diagonal entries. Thus, they generate all real diagonal matrices in  $\mathfrak{d}(\dim S^\lambda)$ . Since a learning ansatz only has real parameters, the following theorem follows.

**Theorem 4.** *Let  $H_P$  be any path-connected Hamiltonian and let  $X_{GZ} \in GZ_n$  denote a real linear combination of*

*elements from  $\{X_i, X_i X_j, X_i X_j X_k, \dots\}$ . Given any  $S^\lambda$ , the subgroup  $H := \langle \exp(i\beta X_{GZ}), \exp(i\gamma H_P) \rangle$  is dense in  $U(\dim S^\lambda)$ . Thus the ansatz constructed by alternating exponentials can approximate any eigenstate of  $H_P$ .*

As we mentioned, this ansatz is impractical because implementing a general element  $X_{GZ}$  would involve non-local high-order products of YJM-elements. These high-order products are used to define the root  $a_{kl}$  with the property that  $a_{k_s l_s} - a_{k_t l_t} \neq 0$  for any  $s \neq t$ . This is the crucial step to establish Lemma 3. Fortunately, we can show that the inequality still holds when restricted to partially-defined roots by first- and second-order products of YJM-elements. Therefore, designing  $H_M$  up to second-order products Eq.(7) is quite enough to generate  $\bigoplus_{(i,j) \in \mathcal{I}} R_{ij}$ . However, only taking YJM-elements cannot guarantee the inequality as shown in Fig.9.

1	2	3	6
4	5		

1	2	3	5
4	6		

1	2	4	6
3	5		

1	2	4	5
3	6		

FIG. 9: Four standard tableaux/Young basis elements/content vectors of (4,2)-irrep of  $S_6$ . Differences between the first two and the last two content vectors are the same.

**Definition 1.** *For any standard Young tableau  $T$  of shape  $(\lambda_1, \dots, \lambda_k)$ , let  $Y_i := X_i + kI$ . The shifted content vector  $\beta_T$  measured by  $Y_i$  only contains positive integers. Using shifted content vector facilitates the following proof. Measuring via second-order product  $Y_i Y_j$ , we obtain an  $(n \times n)$ -component vector  $\beta_T^{(2)}(r, s)$ . It can also be written as a real symmetric matrix  $(\beta_T)^T \beta_T$  and hence called tensor product content vector.*

**Lemma 5.** *Different standard Young tableaux/Young basis elements have different tensor product content vectors. Moreover, let  $T_i, T_j, T_k, T_l$  be four standard Young*

tableaux of size  $n$ . We require that  $T_i \neq T_j$  and  $T_k \neq T_l$ . If all underlying Young diagrams are the same, we further require that  $T_i \neq T_k$  or  $T_j \neq T_l$  (this requirement comes from the computation of roots above). Then

$$\beta_i^{(2)} - \beta_j^{(2)} \neq \beta_k^{(2)} - \beta_l^{(2)}$$

That is, when extended to tensor product content vectors, the differences of unequal standard Young tableaux are still different.

Finally, we can conclude with:

**Theorem 5.** *The subgroup generated by  $Y_k Y_l$  with a path-connected Hamiltonian  $H_P$  is still dense. Since  $Y_k Y_l = (X_k + kI)(X_l + kI) = X_k X_l + k(X_k + X_l) + k^2 I$  and since  $\exp(i\theta I)$  is simply a phase term, a  $S_n$ -CQA ansatz is written as*

$$\begin{aligned} & \cdots \exp(-i \sum_{k,l} \beta_{kl} X_k X_l) \exp(-i\gamma H_P) \\ & \exp(-i \sum_{k,l} \beta'_{kl} X_k X_l) \exp(-i\gamma' H_P) \cdots, \end{aligned} \quad (9)$$

where we redefine  $X_1$  as  $I$  with which any first-order YJM-element  $X_i$  can be written as  $X_i X_1$ .

We present all the proofs for Young diagrams with arbitrary  $SU(d) - S_n$  duality in the SM. Working from the perspective of  $S_n$  also frees us from computing complicated  $SU(d)$  generators.

Consider now the case when  $H_P$  is not path-connected. That is,  $H_P$  is block diagonal (after a possible re-coding of basis elements) in  $S^\lambda$ . It is straightforward to check that Theorem 5 still holds within each sub-block of  $H_P$ . Suppose our task is to find the eigenvector  $v_0$  of  $H_P$  with the lowest eigenvalue of  $H_P$  in  $S^\lambda$ . There is generally no prior knowledge about which sub-block  $v_0$  is living. The brute-force way to find the minimum is by taking a collection of initial states from each of these sub-blocks and applying the theorem repeatedly. One way to do this is by implementing the efficient QST which gives us access to all Young basis elements. The state initialization proposed in Section III B with constant-depth may take a hit (forcing the depth of the circuit to increase) if the problem Hamiltonian is not path-connected. (see Section VI).

### Universality of QAQA

The first proof of the universality of the QAQA ansätze was given in [48], where the authors considered problem Hamiltonian of the first-order and second-order nearest-neighbor interaction. [49] subsequently generalized the result to broader families of ansätze defined by sets of graphs and hyper-graphs. We now describe a new proof based on the techniques developed in this paper that covers novel, broader family of QAQA ansätze. More precisely, we change to the computational basis  $\{|e_i\rangle\}_{i=1}^{2^n}$  in

which all tensor products  $\tilde{Z}_{r_1 \dots r_s} := Z_{r_1} \otimes \cdots \otimes Z_{r_s}$  of Pauli basis can span any diagonal matrix. In the language of Lie algebra,  $Z_i$  generates the Cartan subalgebra  $\mathfrak{d}(2^n)$  of  $\mathfrak{gl}(2^n, \mathbb{C})$ . Roots can be computed by diagonal elements of  $Z_i$  (cf. Lemma 3) which are just spin components of computational basis. We denote by  $H_Z$  the Hamiltonian composed by  $\tilde{Z}_{r_1 \dots r_s}$  and let  $H_X$  be the uniform summation of Pauli  $X$  operators (we do not write its explicit form to avoid any confusion with the notation of YJM-elements). The Hamiltonian  $H_X$  is path-connected under  $\{|e_i\rangle\}$ . Then one can argue similarly as in Theorem 4 that the alternating ansätze generated by  $H_Z$  and  $H_X$  are universal. One may also expect  $H_Z$  being composed by local operators. This holds true, but unlike  $H_Z$  in [48] which contains only nearest neighbor terms  $Z_j Z_{j+1}$ , it is necessary to take all  $\mathcal{O}(n^2)$  terms of second-order product  $Z_k Z_l$  in our proof. The resulting Hamiltonian  $H_Z$  is still simple though and the proof works for both odd and even number of qubits [49]. Moreover, replacing  $H_X$  by any other path-connected Hamiltonian, e.g., antiferromagnetic Heisenberg Hamiltonian [73], still guarantees the universality, and this fact enables one to experiment with a wide range of mixing Hamiltonians. In summary,

**Theorem 6.** *Let  $H_X$  be the uniform summation of Pauli  $X$  operators or any other path-connected Hamiltonian on computational basis, the QAQA-ansatz generated by  $H_X, H_Z = \sum \beta_{kl} Z_k Z_l$  is dense in  $U(2^n)$ , i.e., it is universal.*

### V. RELATION TO ADIABATIC QUANTUM COMPUTING

Similar to the limiting  $p \rightarrow \infty$  behavior of QAQA, our ansatz corresponds to the adiabatic quantum evolution for each  $S_n$  irreducible representation subspace. The standard interpolating Hamiltonian is given by:

$$\begin{aligned} \hat{H}(s) &= sH_p + \sum_{k \leq \ell} (1-s) \beta_{k\ell}(s) X_k X_\ell \\ &= sH_p + (1-s)H_M(s), \end{aligned} \quad (10)$$

where  $s$  ranging from 0 to 1 is the time-parameterized path with  $s(0) = 0$  and  $s(T) = 1$ . In contrast with the standard interpolating Hamiltonian, we set the coupling strength parameters  $\{\beta_{k\ell}\}$  as path dependent I.I.D. random variables drawn from some possibly unknown distribution  $\mathcal{D}$ . Using the Central Limit Theorem, it suffices to draw  $\{\beta_{k\ell}\}$  from normal distributions (when  $n$  is large), say  $\mathcal{N}(0, \sigma)$ . We shall work in  $SU(2)$ - $S_n$  duality but generalization to qudits is straightforward.

Choose an irrep subspace  $S^\lambda$  with the instantaneous ground and first excited states  $|v_0(s)\rangle, |v_1(s)\rangle$  and the spectral gap  $\Delta = \min_{s \in [0,1]} E_1(s) - E_0(s)$ . The adiabatic theorem implies that  $|v_0(s=T)\rangle$  is  $L^2$ - $\epsilon$  close to the ground state of  $H_p$  if:

$$T \gg \frac{|\langle v_1(s) | \partial_s \hat{H}(s) | v_0(s) \rangle|}{\Delta^2}, \quad (11)$$

where:

$$\partial_s \hat{H} = H_p - \sum_{k \leq \ell} \beta_{k,\ell}(s) X_k X_\ell - s \sum_{k \leq \ell} \partial_s \beta_{k,\ell}(s) X_k X_\ell.$$

The quantum evolution in the Heisenberg picture is:

$$U(T) = \mathcal{T} \exp(-i \int_0^T dt \hat{H}(s(t))).$$

Taken  $T = N\Delta t \equiv \Delta t_N$  where  $s(\Delta t_j)$  is constant at this small time increments, the standard Trotterization technique implies that:

$$U(T) \approx \prod_{j=1}^N \exp(-i\Delta t_j s(\Delta t_j)) \prod_{k \leq \ell}^n \exp(-i\Delta t_j (1 - s(\Delta t_j)) \beta_{k,\ell}(\Delta t_j) X_k X_\ell). \quad (12)$$

Setting  $\gamma_j = \Delta t_j s(\Delta t_j)$  and  $\tilde{\beta}_{k,\ell,j} = \Delta t_j (1 - s(\Delta t_j)) \beta_{k,\ell}(\Delta t_j)$ , we recover the  $S_n$ -CQA ansätze at  $p = N$ . The variational parameters  $\{\tilde{\beta}_{k,\ell,j}\}_{k,\ell}$  for the classical optimization corresponds to the randomized coupling strength parameters for the initial Hamiltonian strictly diagonal in the total spin basis elements.

The adiabatic evolution time  $T$  may be exponential if the spectral gap  $\Delta$  is exponentially small as the number of spins grows. There are many works involving techniques to amplify the spectral gap, such as modifying the initial and final Hamiltonian [74, 75], quantum adiabatic brachistochrone [76], and adding non-stoquastic Hamiltonian [77, 78], to name a few. We refer interested readers to [79] for further discussion. Therefore, one may ask whether the path-dependent randomized coupling coefficients would lead to amplification of the spectral gap so that the final evolution time  $T$  can be polynomial bound. In particular, one might need to consider the dynamics of the random path-dependent coupling  $\beta_{k,\ell}(s)$ , such as the Langevin or diffusion processes, supplemented by systems of stochastic differential equations.

The answer to this question will shed light on the existence of a quantum advantage in finding the exact eigenstate of the problem Hamiltonian. Furthermore, by relating it to the adiabatic evolution, similarly to QAOA, this would imply that the  $S_n$ -CQA ansätze enjoys a guaranteed performance improvement as the number of alternating layers  $p$  increases. We leave this as an open question. The success in approximating the sign structure of the ground state in numerical simulation from the  $S_n$ -CQA ansätze may serve as heuristic evidence for such a potential quantum advantage, in addition to the super-exponential quantum speed-up in performing Fourier space convolution in quantum circuits.

## VI. $\mathbb{C}[S_n]$ SYMMETRIES OF $J_1$ - $J_2$ HEISENBERG HAMILTONIAN

The spin-1/2  $J_1$ - $J_2$  Heisenberg model is defined by the Hamiltonian:

$$\hat{H}_p = J_1 \sum_{\langle ij \rangle} \hat{\mathbf{S}}_i \cdot \hat{\mathbf{S}}_j + J_2 \sum_{\langle\langle ij \rangle\rangle} \hat{\mathbf{S}}_i \cdot \hat{\mathbf{S}}_j, \quad (13)$$

where  $\hat{\mathbf{S}}_i = (\hat{S}_i^x, \hat{S}_i^y, \hat{S}_i^z)$  represents the spin operators at each site of a lattice. The symbols  $\langle \dots \rangle$  and  $\langle\langle \dots \rangle\rangle$  indicate pairs of nearest and next-nearest neighbor sites, respectively. The  $J_1 - J_2$  model has been the subject of intense research over its speculated novel spin-liquid phases at frustrated region [80]. The unfrustrated regime ( $J_2 = 0$  or  $J_1 = 0$ ) for the anti-ferromagnetic Heisenberg model is characterized by the bipartite lattices, for which the sign structures of the respective ground states are analytically given by the *Marshall-Lieb-Mattis theorem* [81]. The system is known to be highly frustrated when  $J_1$  and  $J_2$  are comparable  $J_2/J_1 \approx 0.5$  [82] and near the region of two phase transitions from Neel ordering to the quantum paramagnetic phase and from quantum paramagnetic to collinear phase, where no exact solution is known. Moreover, little is known about the intermediate quantum paramagnetic phase – recent evidence of deconfined quantum criticality [83, 84] sparked further interest in studying these regimes. Gaining physical insights in the intermediate quantum paramagnetic phase requires solving the problem of the ground state sign structure the system approaches the phase transition. Recently, there were a number of numerical attempts to address the existence of the U(1) gapless spin liquid phase, using recently the tensor networks [85], restricted Boltzmann Machine (RBM) [86], convolutional neural network (CNN) [50, 51, 87], and graphical neural network (GNN) [88] – all yielding partial progress.

### Global SU(2) Symmetry and Challenges in NQS Ansätze

Taking advantage of the global SU(2) symmetry, we address this problem in a different way: we recast the Hamiltonian in Equation (13) using Equation (3). An immediate consequence is that the resulting Heisenberg Hamiltonian can be expressed in the Young basis where every  $S_n$ -irrep is indexed by the total spin-label  $j$ . Mapping to this basis can be done using the constant-depth circuit state initialization in Section III.C. Using our  $\mathbb{C}[S_n]$  variational ansatz leads to a more efficient algorithm by polynomially reducing the space. In the NISQ application, especially between 10 to 50 qubits, we have much better scaling see Fig.10.

Numerous efforts in applying NQS variational architecture to represent the complicated sign structure in the frustrated regime essentially use the energy as the only criterion for assessing its accuracy. This would result in



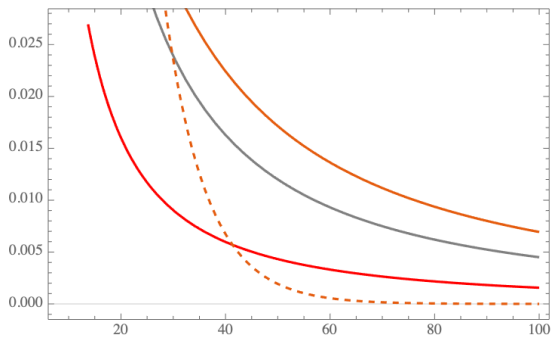


FIG. 10: The scaling properties of small total spin irreps dimension respectively. The graph shows the scale:  $2^n / \text{Dim}(S^\lambda)$  with the partitions  $\lambda_1 = (n/2, n/2)$  (red),  $\lambda_2 = (n/2 + 1, n/2 - 1)$  (grey),  $\lambda_3 = (n/2 + 2, n/2 - 2)$  (orange) The orange dashed line is  $\exp(-n/8)$  the exponential decay. since the plot starts at  $n = 8$ .

the optimized low-energy variational states in frustrated regime still obeying the Marshall sign rules even though the true ground state is likely to deviate from it significantly [51], or breaks the  $SU(2)$  symmetry [50]. The preservation of spatial symmetry has been the core topic of discussion in the literature, with proposed  $C_4$  equivariant CNN. However, on the 2D model Heisenberg model, the spatial symmetry consideration can only reduce the search space redundancy by a constant factor, thus scaling very poorly at even intermediate  $n$ . By reinforcing  $SU(2)$  symmetry, we achieve a polynomial reduction of Hilbert space and ensure the result to be physically reasonable, hence offering a second criterion to assess the variational ansätze.

The number of qubits scaling linearly with the number of qubits naturally circumvent the issue of having generalization property, a crucial property for the NQS ansätze to function [89]. In fact, in Section III, we showed making use of the representation theory of the symmetric group this leads to the super-exponential quantum speed-up. To this end, it is unlikely that any classically trained ansätze are capable to reinforce the global  $SU(2)$  symmetry of the system.

### A. Numerical Simulation

We provide numerical simulations to showcase the effectiveness of the  $S_n$ -CQA ansätze, using JAX automatic differentiation framework [90]. The implementation of the  $S_n$ -CQA ansätze utilizes the classical Fourier space activation by working in the  $S_n$  irreducible representation subspace where the ground state energy lies. This would impact the stability of the numerical simulations, which imply the best-suited models are with 8-16 spins. This bottleneck in computational resource, as shown in Section III, presents no issue for a potential larger-scale implementation on quantum comput-

ers. The benchmarked examples with RBM and Group-equivariant Convolutional Neural Network (GCNN) [91] are drawn from NetKet [92] tutorial <https://www.netket.org/tutorials.html>, which form the baseline comparison. Note that these benchmark algorithms we implemented do not preserve space continuous symmetry such as  $SU(2)$  or  $U(1)$ . For numerical simulation of  $S_n$ -CQA, we perform random initialization of the parameters. We found that the random initialization already returns the energy which is within roughly  $10^{-2}$  precision within ED ground state energy and non-oscillating descents around the ED ground state energy comparing with that of GCNN and RBM. This is likely due to the fact that we used the  $S_n$ -Fourier space activation with real-valued trial wavefunctions with explicit  $SU(2)$  symmetry. We record the optimized energy for the  $S_n$ -CQA ansätze every five iterations, and we set the number of alternating layers  $p = 4$  for the  $3 \times 4$  lattice and  $p = 6$  for the 12-spin Kagome lattice. In the implementation, we shift the Hamiltonian to  $\tilde{H}(\lambda) = H(\lambda) + m 1_{d_\lambda}$  to ensure  $\tilde{H}(\lambda)$  is positive semi-definiteness in the  $S_n$ -irrep specificity by the partition  $\lambda = (\lambda_1, \lambda_2)$  with the total spin label  $j = (\lambda_1 - \lambda_2)/2$  (Section II A), where  $m$  is the total number of transpositions. We only take the real (normalized) part of the wavefunction  $\text{Re}(\psi) = \psi + \psi^*$ . This can be seen as a post-processing step for the realization of  $S_n$ -CQA on a quantum computer. We use the Nesterov-accelerated Adam [93] for the  $S_n$ -CQA optimization with hyper-parameters: betas = [0.99, 0.999]. We also utilize NetKet's ED (Exact Diagonalization) result for the comparison with the exact ground state energy. The ground state is additionally calculated in the Young (Schur) basis by diagonalizing the Heisenberg Hamiltonian  $H(\lambda)$  in the irrep  $\lambda$  where the ground state lives. It is worth mentioning that our optimized ground state is strictly real-valued and has explicitly  $SU(2)$  symmetry, offering the missing yet essential physical interpretation. We provide code and Jupiter notebook in open-access on Github in python. The numerical simulations are run in CPU platform with the 9th Gen 1.4 GHz Intel Core i5 processors.

#### $3 \times 4$ Rectangular Lattice

In frustrated region of  $J_2/J_1 = 0.5$ ,  $J_2/J_1 = 0.8$ , we found that the ground state lives entirely in the total spin 0 irrep, corresponding to the partition  $\lambda = (4, 4)$ . In the case of  $J_2 = 0.5$ , we report that the  $S_n$ -CQA ansätze are able to smoothly converge to the ground state, resulting in the overlap between the ED ground state 0.9973676, with the final optimized ground state energy:  $-5.339714$ , roughly within  $10^{-2}$  precision of the ED ground state energy. For  $J_2 = 0.8$ , the  $S_n$ -CQA returns the optimized energy  $-5.726855$ , within  $10^{-2}$  precision of the ED ground state energy. As a result, the overlap between the ED ground state is 0.9996319. We notice that the  $S_n$ -CQA seem always to converge to the ground state with reasonable good accuracy without the issue of trap-

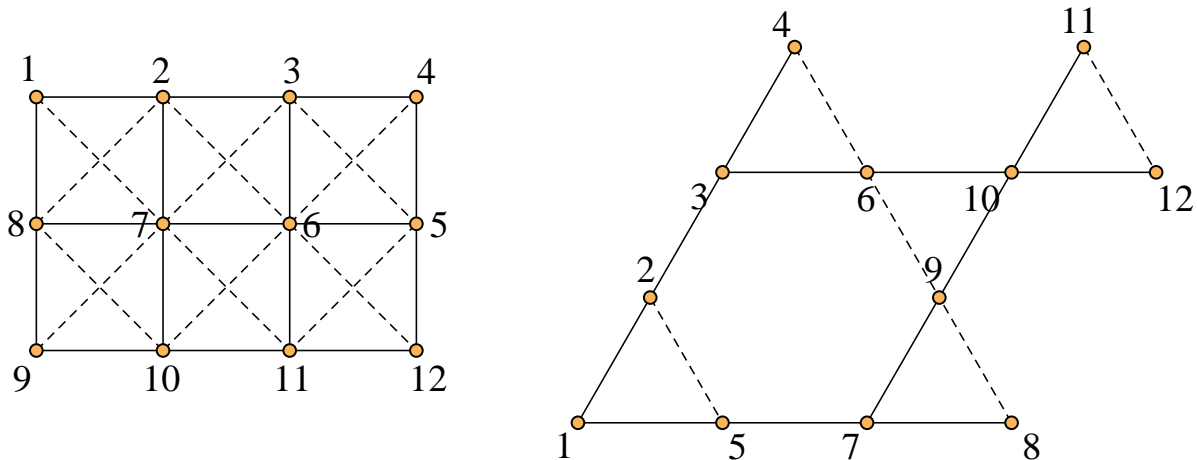


FIG. 11: Rectangular and Kagome lattices.

ping in local minima, regardless of initialization (random initialization from Gaussian is used). The Learning rate used here is 0.002 and 0.001 for the  $S_n$ -CQA respectively. For the GCNN layers in both  $J_2$  values we set the feature dimensions of hidden layers (8, 8, 8, 8) and 1024 samples with the learning rate set for 0.02. For the RBM model, we fix the learning rate 0.02 with 1024 samples.

#### 12-Spin Kagome Lattice

We found by comparing with ED result that the ground state of 12-spin Kagome lattice lives in the total spin 2 irrep, corresponding to partition [8, 4] in  $J_2 = 0$ , which suggests it to be 5-fold degenerate. For the both frustration level  $J_2/J_1 = 0.5$  and  $J_2/J_1 = 0.8$ , the ground state lives in total spin 0 irrep, which appear to be non-degenerate. We aim to learn the ground state for the 12-spin Kagome lattice at  $J_2/J_1 = 0.5$  and  $J_2/J_1 = 0.8$ . In the case of  $J_2/J_1 = 0.5$ , the optimized ground state energy by the  $S_n$ -CQA ansätze at the end of iteration returns  $-4.12269$ , falling roughly within  $10^{-2}$  precision with the ED result. We expect further modifications (for instance, longer iterations, better-suited gradient descent algorithms, increasing  $p$ , etc.) would improve this result to approaching the exact ground state even closer. The overlap between the ED ground state is 0.98525. In the case  $J_2/J_1 = 0.8$ , we have the final optimized energy 4.881405, within roughly  $10^{-2}$  precision from the ED ground state energy. As a result, the overlap is 0.9967997. The performance in terms of both optimized energy and the overlap suffers slightly drawback compared to the learning in the  $3 \times 4$  rectangular lattice. This drop in performance is likely due to the existence of the strong geometric frustration in the antiferromagnetic Heisenberg Kagome lattices. The learning rate is set for 0.001 and 0.002 for the  $J_2/J_1 = 0.5$  and 0.8 respectively. We set the GCNN in both frustration points of feature

dims (8, 8, 8, 8) with 1024 samples. The learning rate in both frustrations is set to be 0.02. The RBM implementation uses 1024 samples with a learning rate 0.02 for both cases.

## DISCUSSION

In this paper, we introduce a framework to design non-Abelian group-equivariant quantum variational ansätze. With the help of the refined Schur-Weyl duality we demonstrated that quantum circuits present a *natural* and theoretically sound option compared to their classical counterparts when performing Fourier space activation. In particular, the quantum Fourier space activation (within PQP+) enjoys a super-exponential quantum speed-up compared with the best-known result in classical FFT over the symmetric group. The density result of the  $S_n$ -CQA ansätze indicates a wide array of other practical problems, in addition to finding the ground state of frustrated magnets. Typical problems would explicitly encode permutation-equivariant structure or exhibit global  $SU(d)$  symmetry. Furthermore, not only do we show that the  $S_n$ -CQA ansätze are dense in every  $S_n$  irrep, but the proof techniques can be used to show the universality of QAOA. We illustrate the remarkable efficacy of our approach by finding the ground state of the Heisenberg antiferromagnet  $J_1$ - $J_2$  spins in a  $3 \times 4$  rectangular lattice and 12-spin Kagome lattice in highly frustrated regimes near the speculated phase transition boundaries. We provided strong numerical evidence that our  $S_n$ -CQA can approximate the ground state with high degree of precision, and strictly respecting  $SU(2)$  symmetry. This opens up new avenues for using representation theory and quantum computing in solving quantum many-body problems.

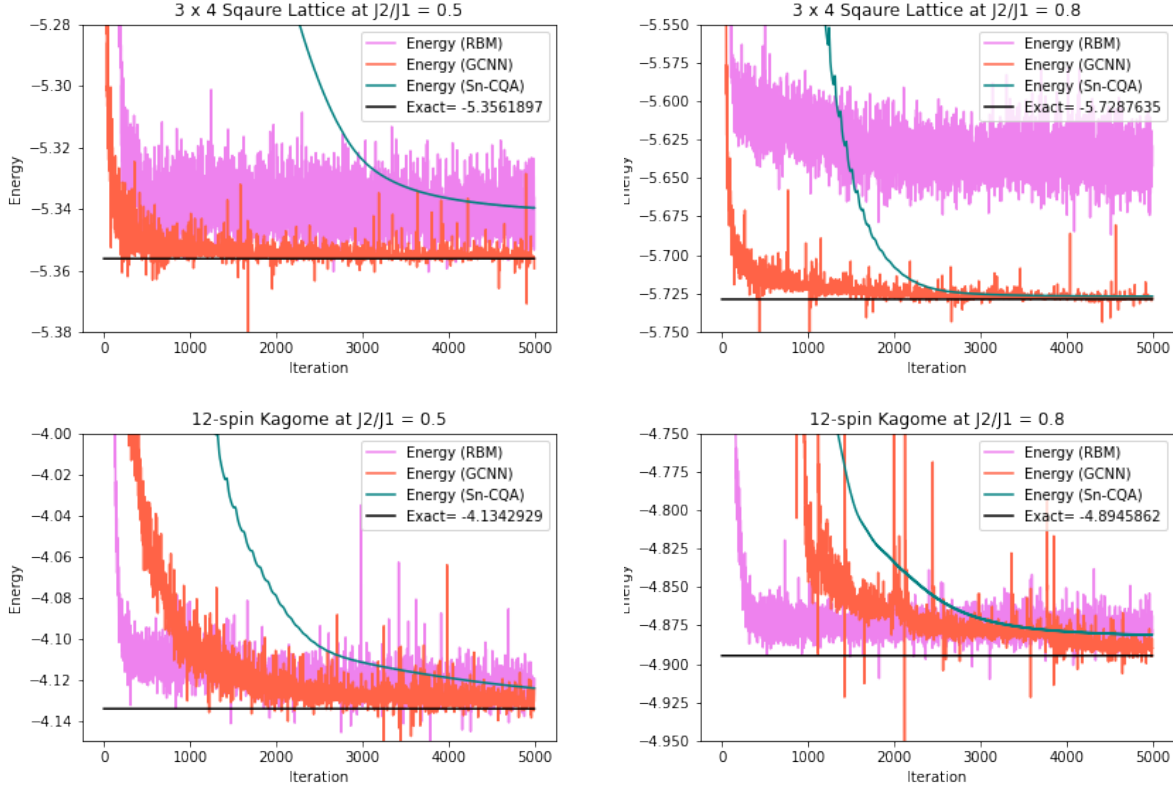


FIG. 12: For the  $3 \times 4$  lattice, in either case, the  $S_n$ -CQA ansätze are able to converge to the ground state with more than 0.99 overlap with the ED ground state. For the Kagome lattice, at both frustration level (a) (down, left) and (b) (down, right), we see that the  $S_n$ -CQA ansätze are able to approach the ground state energy. In particular, the overlap with the ED ground state in (a) is 0.98525 and in (b) is 0.9967997. The above figures indicate that the absence of oscillating behavior in gradient descent and that the  $S_n$ -CQA returns real-valued expectation value strictly above and approaching the exact ground state energy. The numerical results are subject to room for further development, for instance— with better gradient descent algorithms such as to utilize the Hessian— since we have only 200-500 learnable parameters to optimize. Therefore, we expect the performance and convergence rate of  $S_n$ -CQA ansätze to further increase with perhaps more refined tuning.

### Open Problems

We conclude with several interesting open problems: (a) In our work we introduced PQP+ computational model. We would like to find out the extent of its computational power. In particular, it is interesting to investigate whether quantum circuits can (in polynomial time) approximate matrix elements of any  $S_n$  Fourier coefficients. A natural starting place is perhaps based on the density result of  $S_n$ -CQA ansätze in each  $S_n$  irrep by asking if a polynomial bounded number of alternating layers  $p$  are able to approximate any matrix element of  $S_n$  Fourier coefficients. A detailed study of this question will shed some light on the nature and scope of the prospective quantum advantage. (b) It would be important to investigate whether the path-dependent coupling strength parameters  $\beta_{kl}$  lead to potential amplitude amplification of the spectral gap in the adiabatic path. In particular, one might need to address the physical dynamics of

the random path-dependent coupling strengths. (c) More generally, the quantum speed-up we demonstrated here is inherently connected to the PQP+. Are there other quantum speed-ups within this framework? In particular, (b) suggests a possible route related to quantum annealing. Another possible route may have to do with measurement-based quantum advantage. For instance, see [94]. Therefore, one might want to ask if our  $S_n$ -CQA ansätze have other sources of quantum exponential speed-up. (d) Another open direction would be to benchmark the performance of the  $S_n$ -CQA ansätze in various Heisenberg models and to implement the  $S_n$ -CQA ansätze on a quantum device.

### CODE AVAILABILITY

The codes for the numerical simulation can be found at <https://github.com/hanzheng98/Sn-CQA>. The C++ implementation of  $S_n$  operations can be found at <https://github.com/hanzheng98/Sn-CQA>.

//github.com/risi-kondor/Snob2. Data availability is upon request by emailing hanz98@uchicago.edu.

## ACKNOWLEDGEMENT

We thank Liang Jiang, Antonio Mezzacapo, Kristan Temme, Miles Stoudenmire, Wenda Zhou, Alexander Bogatskiy, Hy Truong Son, Horace Pan, Jiequn Han, and

Erik H. Thiede for useful discussions. We thank Chihchan Tien, Christopher Roth, and Giuseppe Carleo for helping in numerical simulation debugging. JL is supported in part by International Business Machines (IBM) Quantum through the Chicago Quantum Exchange, and the Pritzker School of Molecular Engineering at the University of Chicago through AFOSR MURI (FA9550-21-1-0209). SS acknowledges support from the Royal Society University Research Fellowship.

- 
- [1] A. W. Harrow, A. Hassidim, and S. Lloyd, Physical review letters **103**, 150502 (2009).
- [2] N. Wiebe, D. Braun, and S. Lloyd, Physical review letters **109**, 050505 (2012).
- [3] S. Lloyd, M. Mohseni, and P. Rebentrost, Nature Physics **10**, 631 (2014).
- [4] P. Wittek, *Quantum machine learning: what quantum computing means to data mining* (Academic Press, 2014).
- [5] N. Wiebe, A. Kapoor, and K. M. Svore, arXiv e-prints , arXiv:1412.3489 (2014), arXiv:1412.3489 [quant-ph].
- [6] P. Rebentrost, M. Mohseni, and S. Lloyd, Physical review letters **113**, 130503 (2014).
- [7] J. Biamonte, P. Wittek, N. Pancotti, P. Rebentrost, N. Wiebe, and S. Lloyd, Nature **549**, 195 (2017).
- [8] J. R. McClean, S. Boixo, V. N. Smelyanskiy, R. Babbush, and H. Neven, Nature communications **9**, 1 (2018).
- [9] M. Schuld and N. Killoran, Physical review letters **122**, 040504 (2019).
- [10] E. Tang, in *Proceedings of the 51st Annual ACM SIGACT Symposium on Theory of Computing* (2019) pp. 217–228.
- [11] V. Havlíček, A. D. Córcoles, K. Temme, A. W. Harrow, A. Kandala, J. M. Chow, and J. M. Gambetta, Nature **567**, 209 (2019).
- [12] Y. Liu, S. Arunachalam, and K. Temme, Nature Physics , 1 (2021).
- [13] J. Liu, F. Tacchino, J. R. Glick, L. Jiang, and A. Mezzacapo, (2021), arXiv:2111.04225 [quant-ph].
- [14] J. R. McClean, J. Romero, R. Babbush, and A. Aspuru-Guzik, New Journal of Physics **18**, 023023 (2016).
- [15] M. Cerezo, A. Arrasmith, R. Babbush, S. C. Benjamin, S. Endo, K. Fujii, J. R. McClean, K. Mitarai, X. Yuan, L. Cincio, *et al.*, Nature Reviews Physics , 1 (2021).
- [16] E. Farhi, J. Goldstone, and S. Gutmann, “A quantum approximate optimization algorithm,” (2014), arXiv:1411.4028 [quant-ph].
- [17] J. Preskill, Quantum **2**, 79 (2018).
- [18] A. Peruzzo, J. McClean, P. Shadbolt, M.-H. Yung, X.-Q. Zhou, P. J. Love, A. Aspuru-Guzik, and J. L. O’Brien, Nature communications **5**, 1 (2014).
- [19] S. McArdle, S. Endo, A. Aspuru-Guzik, S. C. Benjamin, and X. Yuan, Reviews of Modern Physics **92**, 015003 (2020).
- [20] X. Yuan, J. Sun, J. Liu, Q. Zhao, and Y. Zhou, Phys. Rev. Lett. **127**, 040501 (2021), arXiv:2007.00958 [quant-ph].
- [21] J. Liu, J. Sun, and X. Yuan, (2021), arXiv:2109.05547 [quant-ph].
- [22] E. Farhi, J. Goldstone, S. Gutmann, and L. Zhou, “The quantum approximate optimization algorithm and the sherrington-kirkpatrick model at infinite size,” (2021), arXiv:1910.08187 [quant-ph].
- [23] S. Hadfield, Z. Wang, B. O’Gorman, E. Rieffel, D. Venturelli, and R. Biswas, Algorithms **12**, 34 (2019).
- [24] Y. LeCun, L. Bottou, Y. Bengio, and P. Haffner, Proceedings of the IEEE **86**, 2278 (1998).
- [25] A. Krizhevsky, I. Sutskever, and G. E. Hinton, Advances in neural information processing systems **25**, 1097 (2012).
- [26] K. Simonyan and A. Zisserman, arXiv e-prints , arXiv:1409.1556 (2014), arXiv:1409.1556 [cs.CV].
- [27] C. Szegedy, W. Liu, Y. Jia, P. Sermanet, S. Reed, D. Anguelov, D. Erhan, V. Vanhoucke, and A. Rabinovich, in *Proceedings of the IEEE conference on computer vision and pattern recognition* (2015) pp. 1–9.
- [28] Y. LeCun, Y. Bengio, and G. Hinton, nature **521**, 436 (2015).
- [29] I. Cong, S. Choi, and M. D. Lukin, Nature Physics **15**, 1273–1278 (2019).
- [30] S. P. Jordan, “Permutational quantum computing,” (2009), arXiv:0906.2508 [quant-ph].
- [31] T. Cohen and M. Welling, in *Proceedings of The 33rd International Conference on Machine Learning*, Proceedings of Machine Learning Research, Vol. 48, edited by M. F. Balcan and K. Q. Weinberger (PMLR, New York, New York, USA, 2016) pp. 2990–2999.
- [32] R. Kondor and S. Trivedi, in *Proceedings of the 35th International Conference on Machine Learning* (2018).
- [33] T. S. Cohen, M. Geiger, J. Koehler, and M. Welling, (2017), arXiv:arXiv:1709.04893v2.
- [34] R. Kondor, Z. Lin, and S. Trivedi, in *Advances in Neural Information Processing Systems 31*, edited by S. Bengio, H. Wallach, H. Larochelle, K. Grauman, N. Cesa-Bianchi, and R. Garnett (Curran Associates, Inc., 2018) pp. 10117–10126.
- [35] N. Thomas, T. Smidt, S. M. Kearnes, L. Yang, L. Li, K. Kohlhoff, and P. Riley, Arxiv e-prints **1802.08219** (2018), 1802.08219.
- [36] B. Anderson, T. S. Hy, and R. Kondor, in *Advances in Neural Information Processing Systems 32*, edited by H. Wallach, H. Larochelle, A. Beygelzimer, F. d’Alché-Buc, E. Fox, and R. Garnett (Curran Associates, Inc., 2019) pp. 14510–14519.
- [37] A. Bogatskiy, B. Anderson, J. T. Offermann, M. Roussi, D. W. Miller, and R. Kondor, “Lorentz group equivariant neural network for particle physics,” (2020), arXiv:2006.04780 [hep-ph].
- [38] M. Zaheer, S. Kottur, S. Ravanbakhsh, B. Póczos, R. Salakhutdinov, and A. Smola, (2017), arXiv:1703.06114.



- [39] H. Maron, H. Ben-Hamu, N. Shamir, and Y. Lipman, in *International Conference on Learning Representations* (2019).
- [40] E. H. Thiede, T. S. Hy, and R. Kondor, “The general theory of permutation equivariant neural networks and higher order graph variational encoders,” (2020), arXiv:2004.03990 [cs.LG].
- [41] D. K. Maslen, *Math. Comp* **67**, 1121 (1998).
- [42] M. Clausen and U. Baum, *Mathematics of Computation* **61**, 833 (1993).
- [43] T. Vieijra and J. Nys, *Physical Review B* **104** (2021), 10.1103/physrevb.104.045123.
- [44] A. W. Harrow, arXiv e-prints, quant-ph/0512255 (2005), arXiv:quant-ph/0512255 [quant-ph].
- [45] D. Bacon, I. L. Chuang, and A. W. Harrow, *Phys. Rev. Lett.* **97**, 170502 (2006), arXiv:quant-ph/0407082 [quant-ph].
- [46] H. Krovi, *Quantum* **3**, 122 (2019).
- [47] A. Okounkov and A. Vershik, *Selecta Mathematica* **2**, 581 (1996).
- [48] S. Lloyd, arXiv e-prints, arXiv:1812.11075 (2018), arXiv:1812.11075 [quant-ph].
- [49] M. E. S. Morales, J. D. Biamonte, and Z. Zimborás, *Quantum Information Processing* **19** (2020), 10.1007/s11128-020-02748-9.
- [50] K. Choo, T. Neupert, and G. Carleo, *Physical Review B* **100** (2019), 10.1103/physrevb.100.125124.
- [51] A. Szabó and C. Castelnovo, *Physical Review Research* **2** (2020), 10.1103/physrevresearch.2.033075.
- [52] B. E. Sagan, *The symmetric group*, 2nd ed., Graduate Texts in Mathematics, Vol. 203 (Springer-Verlag, New York, 2001) pp. xvi+238, representations, combinatorial algorithms, and symmetric functions.
- [53] R. Goodman and N. R. Wallach, *Symmetry, Representations, and Invariants* (Springer New York, 2009).
- [54] T. Ceccherini-Silberstein, F. Scarabotti, and F. Tolli, *Representation Theory of the Symmetric Groups* (Cambridge University Press, 2009).
- [55] A. Young, *The Collected Papers of Alfred Young 1873–1940*, edited by G. de Beauregard Robinson (University of Toronto Press, 1977).
- [56] A.-A. Jucys, *Reports on Mathematical Physics* **5**, 107 (1974).
- [57] G. Murphy, *Journal of Algebra* **69**, 287 (1981).
- [58] V. Havlíček and S. Strelchuk, *Physical Review Letters* **121** (2018), 10.1103/physrevlett.121.060505.
- [59] L. C. Biedenharn, *Journal of Mathematical Physics* **4**, 436 (1963).
- [60] R. Pauncz, *The Symmetric Group in Quantum Chemistry* (CRC Press, 2018).
- [61] G. E. Baird and L. C. Biedenharn, *Journal of Mathematical Physics* **4**, 1449 (1963).
- [62] V. Havlíček, S. Strelchuk, and K. Temme, *Physical Review A* **99** (2019), 10.1103/physreva.99.062336.
- [63] R. Kondor and S. Trivedi, “On the generalization of equivariance and convolution in neural networks to the action of compact groups,” (2018), arXiv:1802.03690 [stat.ML].
- [64] R. Kondor, Z. Lin, and S. Trivedi, “Clebsch-gordan nets: a fully fourier space spherical convolutional neural network,” (2018), arXiv:1806.09231 [stat.ML].
- [65] R. Penrose, *Quantum theory and beyond*, 151 (1971).
- [66] N. W. Andrew M. Childs, *Quantum Information and Computation* **12** (2012), 10.26421/qic12.11-12.
- [67] D. W. Berry, A. M. Childs, R. Cleve, R. Kothari, and R. D. Somma, *Physical Review Letters* **114** (2015), 10.1103/physrevlett.114.090502.
- [68] W. Heisenberg, *Zeitschrift für Physik* **49**, 619 (1928).
- [69] D. J. Klein and W. A. Seitz, *International Journal of Quantum Chemistry* **41**, 43 (1992).
- [70] K. Seki, T. Shirakawa, and S. Yunoki, *Physical Review A* **101** (2020), 10.1103/physreva.101.052340.
- [71] A. Anand, P. Schleich, S. Alperin-Lea, P. W. K. Jensen, S. Sim, M. Díaz-Tinoco, J. S. Kottmann, M. Degroote, A. F. Izmaylov, and A. Aspuru-Guzik, “A quantum computing view on unitary coupled cluster theory,” (2021), arXiv:2109.15176 [quant-ph].
- [72] M. Kuranishi, *Nagoya Mathematical Journal* **2**, 63 (1951).
- [73] H. Tasaki, *Physics and Mathematics of Quantum Many-Body Systems* (Springer International Publishing, 2020).
- [74] E. Farhi, J. Goldston, D. Gosset, S. Gutmann, H. B. Meyer, and P. Shor, **11**, 181–214 (2011).
- [75] B. Altshuler, H. Krovi, and J. Roland, *Proceedings of the National Academy of Sciences* **107**, 12446 (2010), <https://www.pnas.org/content/107/28/12446.full.pdf>.
- [76] A. T. Rezakhani, W.-J. Kuo, A. Hamma, D. A. Lidar, and P. Zanardi, *Physical Review Letters* **103** (2009), 10.1103/physrevlett.103.080502.
- [77] L. Zeng, J. Zhang, and M. Sarovar, *Journal of Physics A: Mathematical and Theoretical* **49**, 165305 (2016).
- [78] B. Seoane and H. Nishimori, *Journal of Physics A: Mathematical and Theoretical* **45**, 435301 (2012).
- [79] T. Albash and D. A. Lidar, *Reviews of Modern Physics* **90** (2018), 10.1103/revmodphys.90.015002.
- [80] L. Balents, *Nature* **464**, 199 (2010).
- [81] E. Lieb and D. Mattis, *Journal of Mathematical Physics* **3**, 749 (1962).
- [82] M. Bukov, M. Schmitt, and M. Dupont, *SciPost Physics* **10** (2021), 10.21468/scipostphys.10.6.147.
- [83] A. Nahum, J. Chalker, P. Serna, M. Ortuño, and A. Somoza, *Physical Review X* **5** (2015), 10.1103/physrevx.5.041048.
- [84] L. Wang, Z.-C. Gu, F. Verstraete, and X.-G. Wen, *Physical Review B* **94** (2016), 10.1103/physrevb.94.075143.
- [85] W.-Y. Liu, S.-S. Gong, Y.-B. Li, D. Poilblanc, W.-Q. Chen, and Z.-C. Gu, “Gapless quantum spin liquid and global phase diagram of the spin-1/2  $j_1$ - $j_2$  square antiferromagnetic heisenberg model,” (2021), arXiv:2009.01821 [cond-mat.str-el].
- [86] Y. Nomura and M. Imada, *Physical Review X* **11** (2021), 10.1103/physrevx.11.031034.
- [87] X. Liang, W.-Y. Liu, P.-Z. Lin, G.-C. Guo, Y.-S. Zhang, and L. He, *Physical Review B* **98** (2018), 10.1103/physrevb.98.104426.
- [88] D. Kochkov, T. Pfaff, A. Sanchez-Gonzalez, P. Battaglia, and B. K. Clark, “Learning ground states of quantum hamiltonians with graph networks,” (2021), arXiv:2110.06390 [quant-ph].
- [89] T. Westerhout, N. Astrakhantsev, K. S. Tikhonov, M. I. Katsnelson, and A. A. Bagrov, *Nature Communications* **11** (2020), 10.1038/s41467-020-15402-w.
- [90] J. Bradbury, R. Frostig, P. Hawkins, M. J. Johnson, C. Leary, D. Maclaurin, G. Necula, A. Paszke, J. VanderPlas, S. Wanderman-Milne, and Q. Zhang, “JAX: composable transformations of Python+NumPy programs,” (2018).

- [91] C. Roth and A. H. MacDonald, “Group convolutional neural networks improve quantum state accuracy,” (2021), arXiv:2104.05085 [quant-ph].
- [92] G. Carleo, K. Choo, D. Hofmann, J. E. Smith, T. Westerhout, F. Alet, E. J. Davis, S. Efthymiou, I. Glasser, S.-H. Lin, and et al., *SoftwareX* **10**, 100311 (2019).
- [93] T. Dozat, “Workshop track - iclr 2016 - openreview,” .
- [94] H.-Y. Huang, R. Kueng, and J. Preskill, *Physical Review Letters* **126** (2021), 10.1103/physrevlett.126.190505.

# Supplemental Material: Speeding up Learning Quantum States through Group Equivariant Convolutional Quantum Ansätze

Han Zheng,<sup>1,2,\*</sup> Zimu Li,<sup>2,†</sup> Junyu Liu<sup>\*,3,4,5,‡</sup> Sergii Strelchuk,<sup>2,§</sup> and Risi Kondor<sup>1,6,7,¶</sup>

<sup>1</sup>Department of Statistics, The University of Chicago, Chicago, IL 60637, USA

<sup>2</sup>DAMTP, Center for Mathematical Sciences, University of Cambridge, Cambridge CB30WA, UK

<sup>3</sup>Pritzker School of Molecular Engineering, The University of Chicago, Chicago, IL 60637, USA

<sup>4</sup>Chicago Quantum Exchange, Chicago, IL 60637, USA

<sup>5</sup>Kadanoff Center for Theoretical Physics, The University of Chicago, Chicago, IL 60637, USA

<sup>6</sup>Department of Computer Science, The University of Chicago, Chicago, IL 60637, USA

<sup>7</sup>Flatiron Institute, New York City, NY 10010, USA

(Dated: December 25, 2021)

∗: corresponding author.

In this Supplemental Material, we will provide more mathematical backgrounds and prove theorems given in the main text.

## CONTENTS

I. More facts about Schur-Weyl duality and $S_n$ representation	1
II. Equivalent between Young basis and $SU(d)$ -irrep basis	2
III. Proofs of the density theorem	2
References	6

## I. MORE FACTS ABOUT SCHUR-WEYL DUALITY AND $S_n$ REPRESENTATION

**Lemma I.1.** Any local part  $\hat{S}_i \cdot \hat{S}_j$  constituting a Heisenberg Hamiltonian  $H = \sum_{ij} J_{ij} \hat{S}_i \cdot \hat{S}_j$  can be written as

$$\hat{S}_i \cdot \hat{S}_j = \frac{1}{2}(ij) - \frac{1}{4}I.$$

*Proof.* Let us consider  $\hat{S}_1 \cdot \hat{S}_2$ . Expanded by definition,

$$\hat{S}_1 \cdot \hat{S}_2 = \frac{1}{2}(J_{12}^2 - J_1^2 - J_2^2),$$

where for now the subscripts on  $J^2$  denotes all sites  $J^2$  acting on. Under total spin basis, it is easy to see that

$$J_{12}^2 - J_1^2 - J_2^2 = \begin{pmatrix} 2 & 0 & 0 & 0 \\ 0 & 2 & 0 & 0 \\ 0 & 0 & 2 & 0 \\ 0 & 0 & 0 & 0 \end{pmatrix} - \frac{3}{4}I - \frac{3}{4}I = \begin{pmatrix} \frac{1}{2} & 0 & 0 & 0 \\ 0 & \frac{1}{2} & 0 & 0 \\ 0 & 0 & \frac{1}{2} & 0 \\ 0 & 0 & 0 & -\frac{3}{2} \end{pmatrix}.$$

While

$$(12) = \begin{pmatrix} 1 & 0 & 0 & 0 \\ 0 & 1 & 0 & 0 \\ 0 & 0 & 1 & 0 \\ 0 & 0 & 0 & -1 \end{pmatrix}.$$

∗ hanz98@uchicago.edu

† lizm@mail.sustech.edu.cn

‡ junyuliu@uchicago.edu

§ ss870@cam.ac.uk

¶ risi@cs.uchicago.edu

Therefore,

$$\hat{S}_1 \cdot \hat{S}_2 = \frac{1}{2}(J_{12}^2 - J_1^2 - J_2^2) = \frac{1}{2}((12) - \frac{1}{2}I).$$

This argument holds for any  $i, j$ , hence the proof follows.  $\square$

**Theorem I.2.** Let  $\langle \pi_{\text{SU}(d)} \rangle$  be the collection of all matrices on  $V^{\otimes n}$  generated by  $\pi_{\text{SU}(d)}$  (i.e., taking both linear spans and matrix products) and let  $\langle \pi_{S_n} \rangle$  be defined similarly. Note that  $\langle \pi_{S_n} \rangle$  is just the representation of  $\mathbb{C}[S_n]$ . Let  $M$  be an arbitrary matrix of  $V^{\otimes n}$ . If it commutes with  $\langle \pi_{\text{SU}(d)} \rangle$ , then  $M \in \langle \pi_{S_n} \rangle$ . If it commutes with  $\langle \pi_{S_n} \rangle$ , then  $M \in \langle \pi_{\text{SU}(d)} \rangle$ .

This theorem is proved by the so-called *double commutant theorem*, details can be found in [1].

**Theorem I.3** (Wedderburn Theorem). Given any  $S_n$ -irrep  $S^\lambda$ , let  $\text{End}(S^\lambda)$  denote the collection of linear transformation of  $S^\lambda$ . With respect to any basis, e.g., the Young basis,  $\text{End}(S^\lambda)$  is simply the collection of all  $\dim S^\lambda \times \dim S^\lambda$  matrices. As a vector space, the group algebra  $\mathbb{C}[S_n]$  is isomorphic with the direct sum of  $\text{End}(S^\lambda)$ :

$$\mathbb{C}[S_n] \cong \bigoplus_{\lambda \vdash n} \text{End}(S^\lambda).$$

We emphasize that being different from a  $\text{SU}(d) - S_n$  duality on  $V^{\otimes n}$ , each different  $\lambda$ , i.e., inequivalent  $S_n$ -irrep, appears only once in the above direct sum and the summation takes all kinds of Young diagrams  $\lambda$  of size  $n$ . In any case, restricting to each  $\lambda$ ,  $\pi_{\mathbb{C}[S_n]}$  produces all  $\dim S^\lambda \times \dim S^\lambda$  matrices and hence any matrix commuting with  $\pi_{\mathbb{C}[S_n]}$  should be a scalar.

## II. EQUIVALENT BETWEEN YOUNG BASIS AND $\text{SU}(d)$ -IRREP BASIS

**Lemma II.1.** Under  $\text{SU}(d) - S_n$  duality, sequential coupling Casimir operators commute with YJM-elements.

*Proof.* We prove the case for  $\text{SU}(2)$  for simplicity. For a fixed number  $k \leq n$  of coupled qubits,  $\text{SU}(2)$  has only one Casimir operator  $J_k^2 = (S_x^k)^2 + (S_y^k)^2 + (S_z^k)^2$ . General case for  $\text{SU}(d)$  follows immediately by considering all the  $d - 1$  Casimir operators constructed in [2] simultaneously.

As the Casimir operator,  $J_k^2$  commutes with  $\pi_{\text{SU}(2)}$ . Thus its matrix representation can be expanded by  $\mathbb{C}[S_k]$  by Theorem I.2. On the other hand, restricted to the first  $k$  qubits,  $J_k^2$  commutes with  $\pi_{\mathbb{C}[S_k]}$  because it is generated by  $(\pi_{\text{su}(2)}, (\mathbb{C}^2)^{\otimes k})$ . Hence Wedderburn theorem forces  $J_k^2$  to be a scalar in different  $S_k$ -irreps. Matrices of this form are completely expressible by  $\text{GZ}_k \subset \text{GZ}_n$ . Therefore,  $J_k^2$  commutes with  $X_1, \dots, X_n$ .  $\square$

**Theorem II.2.** The YJM-elements are strictly diagonal under the  $\text{SU}(d)$  irrep basis. Conversely, sequentially coupled Casimir operators are strictly diagonal in the Young basis. Hence the  $\text{SU}(d)$  irrep basis and the Young basis are equivalent.

*Proof.* The proof has two steps, we first show that  $X_i$  is block-diagonal under  $\pi_{\text{SU}(d)}$ , then we verify that it is strict diagonal. We only discuss the  $\text{SU}(2)$ -case for brevity. Obviously, sequential coupling Casimir operators  $J_k^2$  are strictly diagonal under the total spin basis. They are restricted to scalars (spin labels) with respect to the decomposition  $(\mathbb{C}^2)^{\otimes n} = \bigoplus_{\lambda} W_{\lambda}^{\oplus m_{\text{SU}(2), \lambda}}$ . For any fixed YJM-element  $X_i$ , since different copies of  $W_{\lambda}$  must exhibit different eigenvalues (spin labels) under at least one  $J_k^2$  and since  $X_i$  commutes with all these  $J_k^2$ ,  $X_i$  should be block-diagonal with respect to each  $W_{\lambda}$ , no matter they are isomorphic or not.

Furthermore, since by Theorem I.2  $X_i$  commutes with the spin operator  $S_z^n$  whose eigenvalues (spin components) are nowhere identical within any  $\text{SU}(2)$ -irrep,  $X_i$  should be a scalar on each  $W_{\lambda}$ . That is,  $X_i$  is diagonal under the total spin basis which indicates it is also the Young basis [3, 4]. Note that the spin operator  $S_z^n$ , and hence the spin component can be used to distinguish basis states from different copies of any isomorphic  $S_n$ -irrep because they classify different permutation modules as explained in the main text. In the general  $\text{SU}(d)$  case,  $S_z^n$  is generalized to  $\frac{1}{2}d(d-1)$  operators to label these copied states [5]. By the same reason, these operators commute with  $X_i$ . Since each copied state is uniquely labeled by these operators, the second step for  $\text{SU}(d) - S_n$  duality follows.  $\square$

## III. PROOFS OF THE DENSITY THEOREM

**Lemma III.1.** Let  $E_{ij} \in \mathfrak{gl}(d, \mathbb{C})$  be the matrix unit with entry 1 at  $(i, j)$  and 0 elsewhere. Given any matrix  $A$ , let  $\mathcal{I} \subset \{1, \dots, d\} \times \{1, \dots, d\}$  be the index set of  $A$  assigned with nonzero off-diagonal entries  $c_{ij}$ . Then Lie subalgebra generated by  $\mathfrak{d}(d)$  and  $A$  contains

$$\mathfrak{d}(d) \bigoplus_{(i,j) \in \mathcal{I}} R_{ij},$$



where  $R_{ij}$  is the 1-dimensional root space spanned by  $E_{ij}$ .

*Proof.* For any diagonal matrix  $h = \text{diag}(h_1, \dots, h_d) \in \mathfrak{d}(d)$ , the Lie bracket  $[h, E_{kl}] = (h_k - h_l)E_{kl}$  gives the root  $a_{kl}(h) := h_k - h_l$  of  $E_{kl}$  under  $h$ . Let  $h := \sum_i \lambda_i E_{ii}$  with  $\lambda = (\lambda_i)$  being determined later. We define

$$M_1 := [h, A] = \left[ \sum_i \lambda_i E_{ii}, \sum_{k,l \in \mathcal{I}} c_{kl} E_{kl} \right] = \sum_{k,l \in \mathcal{I}} a_{kl}(E_{ii}) \lambda_i E_{kl} = \sum_{k,l \in \mathcal{I}} (a_{kl} \cdot \lambda) E_{kl}.$$

In the second step of the above computation, we omit all possible diagonal elements of  $A$ . This is legal because the Lie bracket of  $h$  with any diagonal part vanishes. Moreover, we set

$$M_2 := [h, [h, A]] = \sum_{k,l \in \mathcal{I}} (a_{kl} \cdot \lambda)^2 E_{kl}, \dots, M_{|\mathcal{I}|} := [h, \dots, [h, A] \dots] = \sum_{k,l \in \mathcal{I}} (a_{kl} \cdot \lambda)^{|\mathcal{I}|} E_{kl}.$$

Note that  $|\mathcal{I}|$  is the number of nonzero off-diagonal elements. Then let us consider the following *Vandermonde matrix*:

$$V(a_{kl} \cdot \lambda) = \begin{pmatrix} 1 & 1 & \dots & 1 \\ a_{k_1 l_1} \cdot \lambda & a_{k_2 l_2} \cdot \lambda & \dots & a_{k_{|\mathcal{I}|} l_{|\mathcal{I}|}} \cdot \lambda \\ \vdots & \vdots & \ddots & \vdots \\ (a_{k_1 l_1} \cdot \lambda)^{|\mathcal{I}|-1} & (a_{k_2 l_2} \cdot \lambda)^{|\mathcal{I}|-1} & \dots & (a_{k_{|\mathcal{I}|} l_{|\mathcal{I}|}} \cdot \lambda)^{|\mathcal{I}|-1} \end{pmatrix}.$$

Viewing  $\mathfrak{gl}(d, \mathbb{C})$  as a  $d \times d$ -dimensional vector space with  $E_{ij}$  as the standard basis, we note that  $V(a_{kl} \cdot \lambda)$  transforms vectors  $\{c_{kl} E_{kl}\}$  to  $\{M_r\}$ . If  $\det V(a_{kl} \cdot \lambda) = (-1)^{|\mathcal{I}|(|\mathcal{I}|-1)/2} \prod_{s < t} (a_{k_s l_s} \cdot \lambda - a_{k_t l_t} \cdot \lambda) \neq 0$ , then it has an inverse and the linear span of  $\{M_r\}$  just equals that of  $\{c_{kl} E_{kl}\}$  which turns out to be  $\bigoplus_{(i,j) \in \mathcal{I}} R_{ij}$  by definition. Basic theory from linear algebra tells us that the union of hyperplanes of finitely-many nonzero vectors, here are  $a_{k_s l_s} - a_{k_t l_t} \neq 0$  as roots, cannot cover the whole vector space. Thus we can always find some  $\lambda$  to fulfill the requirement.  $\square$

The crucial technique of using Vandermonde matrix is adapted from the classical paper [6] on generating semisimple Lie algebra. By Okounkov-Vershik approach [3], a root  $a_{kl}$  in our setting is obtained by all products of YJM-elements. The difference  $a_{k_s l_s} - a_{k_t l_t}$  is always nonzero for roots, but using high order products of YJM-elements leads to a practical problem for ansatz design. Fortunately, we can solve this problem in the setting of  $S_n$ -CQA ansatz as well as of QAOA. The solution is given after Theorem III.4.

**Definition III.2.** Given an arbitrary Hermitian matrix  $H_P$ , let  $\mathcal{G}_{H_P}$  be the underlying indices graph of  $H_P$ . The matrix  $H_P$  is *path-connected* if the associated graph  $\mathcal{G}_{H_P}$  is connected. For instance, the matrix

$$H_P = (E_{14} + E_{23} + E_{35} + E_{45}) + (E_{41} + E_{32} + E_{53} + E_{54})$$

is path-connected. However,

$$H'_P = (E_{14} + E_{23} + E_{55}) + (E_{41} + E_{32} + E_{55})$$

is disconnected. One can see by exchanging rows and columns that  $H'_P$  is block-diagonal. Path-connectedness is also seen in the famous Perron-Frobenius theorem which has lots of applications in graph theory.

**Lemma III.3.** Let  $H_P$  be a path-connected Hamiltonian. Then the generated Lie algebra  $\langle \mathfrak{d}(d), H_P \rangle = \mathfrak{gl}(d, \mathbb{C})$ . Especially, let us consider  $\mathfrak{d}_{\mathbb{R}}(d)$  consisting of all real-valued diagonal matrices. Generated over  $\mathbb{R}$ ,  $\langle i\mathfrak{d}_{\mathbb{R}}(d), iH_P \rangle_{\mathbb{R}} = \mathfrak{u}(d)$ .

*Proof.* By the previous lemma,

$$\mathfrak{d}(d) \bigoplus_{(i,j) \in \mathcal{I}} R_{ij} \subset \langle \mathfrak{d}(d), H \rangle.$$

Given any pair of indices  $i \neq j$ , since the underlying indices graph of  $H_P$  is path connected, we can always find a path  $i = i_0 \rightarrow i_1 \rightarrow \dots \rightarrow i_k \rightarrow i_{k+1} = j$  with no repeating indices for which  $(i_l, i_{l+1}) \in \mathcal{I}$ . Thus

$$E_{ij} = E_{i_0 i_{k+1}} = [\dots [[E_{i_0 i_1}, E_{i_1 i_2}], E_{i_2 i_3}], \dots, E_{i_k i_{k+1}}]$$

belongs to the generated Lie algebra. Since  $\mathfrak{gl}(d, \mathbb{C}) = \mathfrak{d}(d) \bigoplus_{(i,j)} R_{ij}$  for arbitrary  $i \neq j$ , we prove the first statement.

On the other hand, the real Lie algebra  $\langle i\mathfrak{d}_{\mathbb{R}}(d), iH_P \rangle_{\mathbb{R}}$  is definitely contained in  $\mathfrak{u}(d)$ . Since its complexification can be expanded as

$$\langle i\mathfrak{d}_{\mathbb{R}}(d), iH_P \rangle_{\mathbb{R}} + i \langle i\mathfrak{d}_{\mathbb{R}}(d), iH_P \rangle_{\mathbb{R}} = \langle \mathfrak{d}(d), H_P \rangle = \mathfrak{gl}(d, \mathbb{C})$$

and since any matrix from  $\mathfrak{gl}(d, \mathbb{C})$  is uniquely decomposed as the sum of a Hermitian and an skew-Hermitian matrices, we complete the proof.  $\square$

**Theorem III.4.** Let  $H_P$  be any path-connected Hamiltonian and let  $X_{GZ} \in \mathcal{GZ}_n$  denote a real linear combination of elements from  $\{X_i, X_i X_j, X_i X_j X_k, \dots\}$ . Given any  $S^\lambda$ , the subgroup  $H := \langle \exp(i\beta X_{GZ}), \exp(i\gamma H_P) \rangle$  is dense in  $U(\dim S^\lambda)$ . Thus the ansätze constructed by alternating exponentials can approximate any of eigenstate  $H_P$ .

*Proof.* Our aim is to show that  $\bar{H} = U(\dim S^\lambda)$ . Generally,  $H$  may not be a Lie group even it is a subgroup of  $U(\dim S^\lambda)$ . However, after taking closure,  $\bar{H}$  becomes a Lie subgroup of  $U(\dim S^\lambda)$  by Cartan's closed subgroup theorem. Then one can talk about the Lie algebra  $\mathfrak{h}$  of  $\bar{H}$ . By definition,  $\exp(i\beta X_{GZ}), \exp(i\gamma H_P) \in H \subset \bar{H}$ . Thus

$$iX_{GZ} = \left. \frac{d}{d\theta} \right|_{\theta=0} e^{i\theta X_{GZ}}, \quad iH_P = \left. \frac{d}{d\gamma} \right|_{\gamma=0} e^{i\gamma H_P} \in \mathfrak{h}.$$

Since  $\mathfrak{h}$  is a real Lie algebra, it is proper to generate it over  $\mathbb{R}$ . Thus Lemma III.3 tells us that  $\mathfrak{h}$  equals  $\mathfrak{u}(\dim S^\lambda)$ .

Even with the same Lie algebra, we cannot claim immediately that  $\bar{H} = U(\dim S^\lambda)$  because  $U(\dim S^\lambda)$  is not simply connected. Fortunately, some basic results from differential topology come to our rescue. By Cartan's closed subgroup theorem,  $\bar{H}$  is a closed embedded submanifold  $U(\dim S^\lambda)$ . Since  $\mathfrak{h} = \mathfrak{u}(\dim S^\lambda)$ ,  $\dim \bar{H} = U(\dim S^\lambda)$ . Embedded submanifold with the same dimension of its ambient manifold should be open. Therefore,  $\bar{H}$  is both open and closed in the connected group  $U(\dim S^\lambda)$ . They must be identical.  $\square$

**Definition III.5.** For any standard Young tableau  $T$  of shape  $(\lambda_1, \dots, \lambda_k)$ , let  $Y_i := X_i + kI$ . The *shifted content vector*  $\beta_T$  measured by these elements only contains positive integers. Using shifted content vector facilitates the following proof. Measuring via second-order product  $Y_i Y_j$ , we obtain an  $(n \times n)$ -component vector  $\beta_T^{(2)}(r, s)$ . It can also be written as a real symmetric matrix  $(\beta_T)^T \beta_T$  and hence called *tensor product content vector*.

**Lemma III.6.** Different standard Young tableaux/Young basis elements have different tensor product content vector. Moreover, let  $T_i, T_j, T_k, T_l$  be four standard Young tableaux of size  $n$ . We require that  $T_i \neq T_j$  and  $T_k \neq T_l$ . If all underlying Young diagrams are the same, we further require that  $T_i \neq T_k$  or  $T_j \neq T_l$  (this requirement comes from the computation of roots above). Then

$$\beta_i^{(2)} - \beta_j^{(2)} \neq \beta_k^{(2)} - \beta_l^{(2)}$$

That is, when extended to tensor product content vectors, the differences of different standard Young tableaux are still different.

*Proof.* The first statement follows by the one-to-one correspondence between Young basis elements and content vectors [3, 4]. To prove the later one, we first look at differences of shifted content vectors

$$\beta_i - \beta_j, \quad \beta_k - \beta_l.$$

If they are different, then we finish the proof.

Suppose then  $\beta_i - \beta_j = \beta_k - \beta_l$ . Since  $\beta_k - \beta_l \neq 0$ ,

$$\beta_i - \beta_j = \beta_k - \beta_l \neq \beta_l - \beta_k.$$

Thus there must be some integer  $r \in \{1, \dots, n\}$  such that

$$\beta_i(r) - \beta_j(r) \neq \beta_l(r) - \beta_k(r) \Leftrightarrow \beta_i(r) + \beta_k(r) \neq \beta_j(r) + \beta_l(r).$$

If  $\beta_i(r) - \beta_k(r) = \beta_j(r) - \beta_l(r) \neq 0$ , then

$$\begin{aligned} \beta_i^{(2)}(r, r) - \beta_k^{(2)}(r, r) &= (\beta_i(r) - \beta_k(r)) (\beta_i(r) + \beta_k(r)) \\ &\neq (\beta_j(r) - \beta_l(r)) (\beta_j(r) + \beta_l(r)) = \beta_j^{(2)}(r) - \beta_l^{(2)}(r) \\ \implies \beta_i^{(2)}(r, r) - \beta_j^{(2)}(r, r) &\neq \beta_k^{(2)}(r, r) - \beta_l^{(2)}(r, r) \implies \beta_i^{(2)} - \beta_j^{(2)} \neq \beta_k^{(2)} - \beta_l^{(2)}. \end{aligned}$$

Suppose  $\beta_i(r) - \beta_k(r) = \beta_j(r) - \beta_l(r) = 0$  for all  $r$  such that  $\beta_i(r) + \beta_k(r) \neq \beta_j(r) + \beta_l(r)$ , i.e.,  $\beta_i(r) = \beta_k(r)$  and  $\beta_j(r) = \beta_l(r)$ . Since  $\beta_i - \beta_j = \beta_k - \beta_l \neq 0$ ,

$$\beta_i(r) - \beta_j(r) = \beta_k(r) - \beta_l(r) \neq 0, \text{ i.e., } \beta_i(r) \neq \beta_j(r), \beta_k(r) \neq \beta_l(r).$$

Since  $T_i \neq T_k$  (otherwise,  $T_j$  must be different from  $T_l$  and that finishes the proof), there must be some  $s$  such that  $\beta_i(s) \neq \beta_k(s)$ . Again since  $\beta_i - \beta_j = \beta_k - \beta_l$ ,  $\beta_j(s) \neq \beta_l(s)$ . Since shifted content vectors only take positive integers as their components,

$$\begin{aligned} \beta_i(r)\beta_i(s) - \beta_k(r)\beta_k(s) &= \beta_i(r)(\beta_i(s) - \beta_k(s)) \neq 0 \\ &\neq \beta_j(r)(\beta_i(s) - \beta_k(s)) = \beta_j(r)(\beta_j(s) - \beta_l(s)) = \beta_j(r)\beta_j(s) - \beta_l(r)\beta_l(s) \\ \implies \beta_i^{(2)}(r, s) - \beta_j^{(2)}(r, s) &= \beta_i(r)\beta_i(s) - \beta_j(r)\beta_j(s) \\ &\neq \beta_k(r)\beta_k(s) - \beta_l(r)\beta_l(s) = \beta_k^{(2)}(r, s) - \beta_l^{(2)}(r, s). \end{aligned}$$

This finishes the proof.  $\square$

Combining Lemma III.6 with Lemma III.1,  $\langle iY_k Y_l, H_P \rangle$  can generate all the off-diagonal root spaces  $R_{ij}$  if  $H_P$  is path-connected. To complement the missing diagonal elements ( $iY_k Y_l$  is not enough to generate whole  $\text{GZ}_n$ ), we note that  $[E_{ij}, E_{ji}] = E_{ii} - E_{jj}$ . Thus all traceless diagonal matrices can be generated from  $\langle iY_k Y_l, H_P \rangle$ . Since, for instance,  $X_2$  is diagonal with a nonzero trace, all diagonal matrices can be generated. In conclusion, we obtain the following theorem.

**Theorem III.7.** *The subgroup generated by  $Y_k Y_l$  with a path-connected Hamiltonian  $H_P$  is still dense. Since  $Y_k Y_l = (X_k + kI)(X_l + kI) = X_k X_l + k(X_k + X_l) + k^2 I$  and since  $\exp(i\theta I)$  is simply a phase term, a  $S_n$ -CQA ansatz is written as*

$$\cdots \exp\left(-i \sum_{k,l} \beta_{kl} X_k X_l\right) \exp(-i\gamma H_P) \exp\left(-i \sum_{k,l} \beta'_{kl} X_k X_l\right) \exp(-i\gamma' H_P) \cdots,$$

where we redefine  $X_1$  as  $I$  with which any first-order YJM-element  $X_i$  can be written as  $X_i X_1$ .

To prove the universality of QAOA and reuse the above method on Pauli  $Z$  matrices and computational basis  $\{|e_i\rangle\}$ , we need to redefine Cartan subalgebra and roots. It is well-known that all diagonal Pauli basis elements  $\tilde{Z}_{r_1 \dots r_s} := Z_{r_1} \otimes \cdots \otimes Z_{r_s}$  are able to span any diagonal matrix under  $\{|e_i\rangle\}$  which in turn forms the Cartan subalgebra of  $\mathfrak{gl}(\mathbb{C}, 2^n)$ . We denote by  $\beta_i(j)$  the eigenvalue of  $|e_i\rangle$  measured by  $Z_j$ . Let  $E_{kl}$  be the matrix unit as in Lemma III.1 but under  $\{|e_i\rangle\}$ . The root  $a_{kl}$  of  $E_{kl}$  is given by

$$a_{kl}(j)E_{kl} = \text{ad}_{Z_j}(E_{kl}) = (\beta_k(j) - \beta_l(j))E_{kl}.$$

High order components of  $a_{kl}$  under  $\tilde{Z}_{r_1 \dots r_s}$  are obtained by products. With all these substitutions, Lemma III.1, Lemma III.3 and Theorem III.4 follow straightforward. We now examine that a local Hamiltonian  $H_Z = \sum \beta_{kl} Z_k Z_l$  consisting of first- and second-order product of Pauli  $Z$  ( $Z_0 = I$ ) also guarantees the universality. With the same spirit of Lemma III.6, we have

**Lemma III.8.** *Let  $v$  be any computational basis element. Then for any  $u_1 \neq v_1, u_2 \neq v_2$  (if  $u_1 = u_2$ , we require  $v_1 \neq v_2$  and vice versa),*

$$\beta_{u_1}^{(2)} - \beta_{v_1}^{(2)} \neq \beta_{u_2}^{(2)} - \beta_{v_2}^{(2)}.$$

*Proof.* One can take this lemma as a corollary of Lemma III.6 where content vectors are replaced by eigenvalues of  $Z_j$ . Since they only take values from  $\{\pm 1\}$ , there is a more straightforward way towards the proof by induction. Suppose the statement is true for  $n - 1$  qubits. Let  $u_1, v_1, u_2, v_2$  be distinct computational basis elements from the  $n$ -qubit system. Possible assignments of their spins of the last qubit are listed in the following:

$$\begin{array}{cccccc} (0, 0, & 0, 0), & (0, 0, & 1, 1), & (1, 1, & 0, 0), & (1, 1, & 1, 1), \\ (0, 1, & 0, 1), & (1, 0, & 1, 0), & (0, 1, & 1, 0), & (1, 0, & 0, 1), \\ (0, 0, & 0, 1), & (0, 0, & 1, 0), & (0, 1, & 0, 0), & (1, 0, & 0, 0), \\ (0, 1, & 1, 1), & (1, 0, & 1, 1), & (1, 1, & 0, 1), & (1, 1, & 1, 0). \end{array}$$

The last ten cases can be confirmed immediately as differences of eigenvalues measured by  $Z_n$  on the last qubit are different. We need to analyze the cases like  $(0, 0, \quad 1, 1)$ . Deleting the last qubits, Deleting the last qubits, suppose then  $u_1 = u_2$  and  $v_1 = v_2$ . Since we require  $u_1 \neq v_1, u_2 \neq v_2$ , there exists some  $i < n$  such that  $\beta_{u_1}(i) - \beta_{v_1}(i) = \beta_{u_2}(i) - \beta_{v_2}(i) \neq 0$ . Then their eigenvalues of  $Z_i Z_n$  will provide the difference. If  $u_1 \neq u_2$  or  $v_1 \neq v_2$ , then by induction, we obtain the proof.  $\square$

Finally we have:

**Theorem III.9.** *Let  $H_X$  be the uniform summation of Pauli  $X$  operators or any other path-connected Hamiltonian on computational basis, the QAOA-ansatz generated by  $H_X, H_Z = \sum \beta_{kl} Z_k Z_l$  is dense in  $\text{U}(2^n)$ , i.e., it is universal.*

- 
- [1] R. Goodman and N. R. Wallach, *Symmetry, Representations, and Invariants* (Springer New York, 2009).
  - [2] L. C. Biedenharn, *Journal of Mathematical Physics* **4**, 436 (1963).
  - [3] A. Okounkov and A. Vershik, *Selecta Mathematica* **2**, 581 (1996).
  - [4] T. Ceccherini-Silberstein, F. Scarabotti, and F. Tolli, *Representation Theory of the Symmetric Groups* (Cambridge University Press, 2009).
  - [5] G. E. Baird and L. C. Biedenharn, *Journal of Mathematical Physics* **4**, 1449 (1963).
  - [6] M. Kuranishi, *Nagoya Mathematical Journal* **2**, 63 (1951).